journal of the international meteor organization

WGN

38:5
october 2010

Conference
Video meteors
Perseus-Auriga meteors

ISSN 1016-3115

WGN Vol. 38, No. 5, October 2010, pp. 135 – 174

Administrative

Conferences

Ongoing meteor work

Front cover photo

A bright Perseid of about −9 magnitude was captured at a Youth astronomical research camp MART 2010 in Medvedje Brdo, Slovenia. The image was taken on 2010 August 12 at 02^h11^m UT using a Nikon D90 camera with an 18 mm lens at $f/3.5$, ISO 1600, exposure 102 seconds. Photo courtesy: Jure Atanackov.

Writing for WGN This Journal welcomes papers submitted for publication. All papers are reviewed for scientific content, and edited for English and style. Instructions for authors can be found in WGN **31:4**, 124–128, and at `http://www.imo.net/articles/writingforwgn.pdf` .

Cover design Rainer Arlt

Legal address International Meteor Organization, Mattheessensstraat 60, 2540 Hove, Belgium.

Editorial – Conference and the Orionids

Javor Kac

September and October have again been busy months for meteor observers.

In September I attended the International Meteor Conference in Armagh, Northern Ireland. This has again been an amazing experience for me.

First, exploring a region I have never visited before is great by itself. While coming to the country was quite easy – I flew from Ljubljana to Belfast via London – it was quite hard to organize other details such as local transport and accommodation before or after the conference. I ended up hiring a car together with Mitja Govedič, another participant and fellow observer from Slovenia. It was a challenge for me to drive on the left side of the road for the first time, but we survived about 400 miles on the road. In any case, hiring a car was a great choice as we could see much of the country, including marshes, lakes, historic sites, nice scenic views from the mountain passes and the northern coast with astonishing cliffs, including the Giant's Causeway.

Second, and most importantly, it is always nice to meet fellow meteor observers and others who work in meteor astronomy in person. That way, it is much more practical to exchange views and experiences, plan new projects, etc. One fine example from this year's Conference was Sirko Molau who was answering questions related with video meteor observing and the recognition software MetRec to many interested participants one whole evening. He also accepted many suggestions to improve the software and even changed the source code live at the site to implement some ideas.

Figure 1 – Tolis Christou demonstrating the 10-inch Grubb refractor at the Armagh Observatory.

Finally, I was pleased we were able to explore the Armagh Observatory and enjoy the hospitality of the staff. Many fine vintage instruments are hosted by the institution, including a working example of 10 inch Grubb refractor, installed in 1885 (Figure 1). I was amazed to see how well the Observatory activities are embedded into the local environment. However, given the long tradition, this should come as no surprise.

And there is still more exciting news: the Proceedings of IMC 2008 in Šachtička, Slovakia were brought to the Armagh conference and distributed to delegates. The papers of the Proceedings are listed on page 144. If you were not present at the Conference in Slovakia but would like to have the Proceedings, see the inside back cover or the IMO website for details.

Another personal recollection of the Conference is presented in an article by Vaibhav Savant from India (see page 142).

October brought another enhanced maximum of the Orionids. Their activity was mostly obscured by the bright moonlight. Despite the adverse conditions and variable weather, I was able to observe for a couple of hours in the morning of October 21. With 50 Orionids and 69 meteors in total, I was not disappointed. I also covered some more nights, observing away from the maximum (and the moonlight). The preliminary activity graph at the IMO live pages shows the Orionids peaked at ZHR about 40 this year.

IMO bibcode WGN-385-editorial NASA-ADS bibcode 2010JIMO...38..135K

Erratum: Meteor Trajectory from Multiple Station Head Echo Doppler Observations

The WGN Editorial Team

In the August issue of WGN, Journal of the International Meteor Organization, we published an article describing a method for determining a meteor's trajectory from its head echo Doppler signature (Steyaert et al., 2010). We regret that there was an error in typesetting Equation (12). The correct rendition of Equation (12) is as follows:

$$\begin{bmatrix} \sum_i A_i^2 & \sum_i A_iB_i & \sum_i A_iC_i \\ \sum_i A_iB_i & \sum_i B_i^2 & \sum_i B_iC_i \\ \sum_i A_iC_i & \sum_i B_iC_i & \sum_i C_i^2 \end{bmatrix} \begin{bmatrix} v_x \\ v_y \\ v_z \end{bmatrix} = \begin{bmatrix} \sum_i Doppl_{Obsi}A_i \\ \sum_i Doppl_{Obsi}B_i \\ \sum_i Doppl_{Obsi}C_i \end{bmatrix} \tag{12}$$

We sincerely apologize to our readers.

References

Steyaert C., Verbelen F., and the VVS Beacon Observers (2010). "Meteor trajectory from multiple station head echo Doppler observations". *WGN, Journal of the IMO*, **38:4**, 123–129.

IMO bibcode WGN-385-erratum NASA-ADS bibcode 2010JIMO...38..136E

Letter — Meteors in Australian Aboriginal Dreamings

Roberto Gorelli [1]

I read the article "Meteors in Australian Aboriginal Dreamings" by Duane W. Hamacher and Ray P. Norris, published in WGN (Hamacher & Norris, 2010). I think that it is a very good work, and I hope that this work will be followed by a complete recording of all Aboriginal histories relating to the meteoritical sciences.

On the specific article of Hamacher and Norris, I want to say that perhaps I did not read the entire article with close attention but the Aboriginal has certainly witnessed one or more meteoritical craters among the many that exist in Australia. In the book Meteorites by Fritz Heide (Heide, 1964) there is written:

page 37–38 [on the Henbury meteor crater field]

> "It is again significant that the Australian aborigines do not camp in the vicinity. They call them 'chindu chinna waru chingi yabu' which means approximately sun-trail-fire-devil-stone. Here too this giant meteorite seems to have fallen as late as the age of man."

Therefore the Aboriginals must have seen this fall and probably other falls during their 50 000 years of history.

As is occurring in Italy, and I think in many other countries around the world, we are losing nearly all oral histories that contain many interesting topics of all types, historical, linguistic, scientific, etc. In many cases these histories are not written, so the death of a man or woman that knows them is also the death of the knowledge of this history.

I ask all readers of WGN in all countries to begin recording these histories, as McBeath and many others are doing.

References

Hamacher D. W. and Norris R. P. (2010). "Meteors in Australian Aboriginal dreamings". *WGN, Journal of the IMO*, **38:3**, 87–98.

Heide F. (1964). *Meteorites*. University of Chicago Press, Chicago. Translated from the second German edition (Berlin, 1957) by Edward Anders and Eugene R. DuFresne.

[1] Via di Val Favara Pal.B 72, I-00168 Roma, Italy.

IMO bibcode WGN-385-gorelli-letter NASA-ADS bibcode 2010JIMO...38L.136G

From the Treasurer — IMO Membership/WGN Subscription Renewal for 2011

Marc Gyssens

We invite all our members/subscribers to renew for 2011. The fees are as tabulated below. We are happy that we can offer WGN at the same cost as last year. From 2011 onwards, we also offer an electronic-only subscription at 5 euros or 10 dollars less than the standard rate.

IMO Membership/WGN Subscription 2011				
Electronic + paper with surface mail delivery:		€26		US$ 39
Electronic + paper with airmail delivery (outside Europe only):		€49		US$ 69
Electronic only:		€21		US$ 29
Supporting membership:	add	€26	add	US$ 39

It is possible to renew for two years by paying double the amount.

General payment instructions can be found on the IMO's website, `http://www.imo.net`. Members and subscribers who have not yet renewed will find enclosed a leaflet with payment instructions that apply to their geographical region. Please follow these instructions! Choosing the most appropriate payment method results in low or even no additional costs for you as well as the IMO. The IMO strives to keeping these costs low in order to control the price of the journal!

When you renew, give a few minutes of thought to becoming a **supporting member**. Every year, the IMO helps active meteor workers to attend the annual International Meteor Conference, who would otherwise not have been able to come. Our ability to provide this help depends primarily on the gifts we receive from supporting members!

Another way to help meteor workers with limited funds is to offer them a gift subscription.

We already thank all our members that will renew for their continued trust in our Organization!

One final request: every year, a lot of members renew late. As a consequence, back issues that already appeared have to be sent out to these members. Please support our volunteers in their bimonthly effort to have WGN shipped to you by renewing promptly! Thank you for your understanding and cooperation!

IMO bibcode WGN-385-gyssens-renewals NASA-ADS bibcode 2010JIMO...38..137G

In Memoriam Bertil Anders Lindblad (1921 – 2010)

Paul Roggemans

Received 2010 October 24

Bertil Anders Lindblad, born on June 11, 1921, passed away on October 9, 2010, 89 years old. In 1989, he became the first Honorary Member of the International Meteor Organization (IMO) in recognition of his crucial support for the foundation of the IMO.

As a scientist, Bertil Lindblad chose to dedicate his talents to the professionally rather unpopular topic of meteor astronomy. Consequently, he was not the kind of scientist looking for sensational discoveries or newspaper headlines. When Lindblad started his career as a researcher towards the end of the 1940s, meteoroid stream structures and dynamics were still largely unexplored. Upcoming new observing techniques such as the use of radar and advanced meteor cameras challenged meteor astronomers to understand the physics of the upper atmosphere and its interaction with the smallest particles of the Solar System.

The first publication by Bertil that came to my hands was a paper published in *Meddelande från Lunds Astronomiska Observatorium* called "A Radar Investigation of the Delta Aquarid Meteor Shower of 1950," published in 1952. Radar observing was very new at that time, and the δ-Aquariids were a rather remarkable target for this observing technique. The observing took place at the Onsala Wave Propagation Observatory managed by the Research Laboratory of Electronics of the Chalmers University of Technology. Contrary to other radar meteor scientists such as McKinley and the Jodrell bank team, Bertil Lindblad compared radar work to previous visual observations from a different point of view than the typical theoretical approach of the physicists.

In 1953, an experiment took place in an attempt to correlate the radar and visual observations of the 1953 Perseids. Bertil Lindblad participated himself as a visual meteor observer and thus was one of the rather few professional meteor astronomers that actually did observe meteors and did not just work from a purely theoretical point of view. This experiment was repeated in 1955 and later years, and inspired some very detailed analyses and subsequent papers. Also, when Lindblad noticed a bright fireball on January 9, 1954, he collected witness reports and analyzed the path and orbit in detail. This interest and dedication to visual meteor observations is reflected in papers published in the *Smithsonian Contributions to Astrophysics* later in the 1960s. In the 1970s, he considered typical aspects of visual observing, such as the discrepancies in visual magnitude estimates by visual observers, studied in cooperation with the famous Slovak meteor researcher, Jan Štohl (1932–1993).

Radar meteor research also had some spin-offs in terms of the study of the Earth's atmosphere. Lindblad studied the solar cycle variations in atmospheric density as deduced from meteor observations. As the observational data extended over longer periods such as 1953–1966, long term variation could be considered in mesosphere and lower thermosphere density. In 1967, Lindblad investigated micrometeorite impacts from a sounding rocket during a noctilucent cloud display.

As computers became available towards the end of the 1960s, meteoroid stream searches became feasible using large numbers of available accurate meteoroid orbits. This opened new perspectives for studying the different types of streams and the association of individual orbits with these streams. The stream search projects led to the awareness that more precise orbital data were needed to satisfy the statistical requirements of this study. Although the need was obvious, it would take many years more before an official data center became a reality, a project to which Bertil Lindblad committed himself personally.

From 1973 to 1976, Bertil Anders Lindblad served as President of IAU Commission 22. A suggestion by this Commission in 1976 certainly contributed to getting the IAU Meteor Orbit Center of Lund established by the IAU General Assembly in 1982. This meteor orbit data center still serves as a major reference.

In 1986, Bertil Lindblad and Iwan Williams were asked by Pulat Babadzhanov (then Chairman of IAU Commission 22) to participate at the International Meteor Conference (IMC) in Hingene, Belgium. By then, most meteor observing groups had become aware that standard reporting formats and methodologies were required to make amateur meteor observing worthwhile. A detailed proposal and complete observing handbook were prepared during the months before this IMC in order to have a round table at the IMC and reach a consensus on this matter. The presence of the two IAU experts was not just symbolic. In 1983, Bertil Lindblad had published a paper on the structure of the Perseid stream in the *Proceedings of the Asteroids, Comets and Meteors Conference (ACM)*, using older Onsala radar data. Another paper on this topic was presented shortly before the 1986 IMC at *ACM II*. Analyzing the Perseid activity in order to map the stream structure like Lindblad did was exactly what amateur meteor observers could achieve, on condition that their observation could be calibrated, and the observing methods and reporting formats used would allow this. In spite of this round table's careful preparation by the present author, George Spalding of the BAA Meteor Section, and several other visual observers, a few amateurs remained unconvinced of the benefits of such an approach. It was precisely Bertil Lindblad who encouraged me to ignore their criticism and to go ahead with those interested. The analysis method used for radar Perseid rates was the main inspiration to set up the data format and the first analyzing routines of the

IMO bibcode WGN-385-roggemans-lindblad NASA-ADS bibcode 2010JIMO...38..138R

Visual Meteor Database (VMDB) in 1988. One of the very first results obtained with the newly created VMDB was a remarkably detailed activity profile for the 1988 Perseids with a distinct double peak. This discovery would lead to the prediction by the IMO of a Perseid outburst, and, eventually, indirectly contribute to the rediscovery of Comet 109P/Swift-Tuttle.

At the *ACM III* meeting in Uppsala in 1989, the foundation of the International Meteor Organization was welcomed by the professional meteor astronomers as a most important development for future amateur-professional cooperation. Before 1988, the amateur meteor observing community was divided into many local groups, some competing in a rather destructive way, and all producing statistically too few and incomparable results due to incompatible observing methodologies, or even the lack of them. Bertil Lindblad promoted the IMO with his colleagues so that the newly founded amateur organization became well accepted by the professional community.

In 1992, a large number of leading professional meteor astronomers participated at the IMC in Smolenice, Slovakia. This was the first time that so many professionals attended an amateur meteor conference. Likewise, a previously unseen number of amateurs participated in the professional *Meteoroids* conference, immediately after the IMC.

Figure 1 – Eight IAU Commission 22 Chairmen: From left to right, L. Kresák (1961), P.D. Babadzhanov (1985–1988), Z. Ceplecha (1967–1970), I.P. Williams (1993–1997), O.I. Bel'kovich (1982–1985), B.A. Lindblad (1973–1976), W.G. Elford (1979–1982), C.S.L. Keay (1988–1991) and J. Štohl (1991–1993).

The last time I met Bertil Lindblad was at the *ACM* conference in Versailles, France in 1996. By that time, the IMO was well established and the standardized observing methodology had proven its reliability much to the delight of Bertil. The detailed meteoroid stream activity profiles that the IMO derived from visual observations worldwide and the meteor shower radiant analyses from the IMO Video Camera Network covered the main topics of Lindblad's meteor research during his long career. He continued this research long after he officially retired, and published several more papers after the 1980s. He maintained his office at the Lund Observatory in Sweden until his death.

Bertil Lindblad provided invaluable advice and support for the foundation of the IMO, be it in a very discrete way. We will always remember him as a very modest and friendly person, with a lot of sympathy for amateur meteor astronomers in general and the IMO in particular. The IMO is forever indebted to Bertil Lindblad for his dedication to meteor astronomy and his unwavering support of the amateur community.

Acknowledgement

The author thanks Pavel Spurný for providing information on the successive chairmen of IAU Commission 22.

This contribution was based on a literature survey. The list below is only a selection and not a complete biography of the papers published by Bertil Anders Lindblad.

References

Lindblad B.A. (1952). "A radar investigation of the Delta Aquarid meteor shower of 1950". *Medd. Lund Obs.*, Ser. I, **179**, 1–27.

Lindblad B.A. (1953). "The peculiar orbit of the Delta Aquarid meteors". *Medd. Lund Obs.*, Ser. I, **183**, 157–159.

Lindblad B.A. (1956). "Combined visual and radar observations of Perseid meteors". *Medd. Lund Obs.*, Ser. I, **189**, 1–98.

Lindblad B.A. (1960). "The radiant and orbit of a bright fireball". *Medd. Lund Obs.*, Ser. I, **196**, 495–516.

Lindblad B.A. (1962). "Combined visual and radar observations of Perseid meteors". *Medd. Lund Obs.*, Ser. I, **198**, 1–38.

Lindblad B.A. (1963). "Relation between visual magnitudes of meteors and the durations of radar echoes". *Smithson. Contr. Astrophys.*, **7**, 27–39.

Hawkins G.S., Lindblad B.A., Southworth R.B. (1964). "The velocity of faint meteors". *Smithson. Contr. Astrophys.*, **8**, 133–139.

Lindblad B.A. (1967a). "Luminosity function of sporadic meteors and extrapolation of influx rate to micrometeorite region" *Smithson. Contr. Astrophys.*, **11**, 171–180.

Lindblad B.A. (1967b). "Solar cycle variations in atmospheric density as deduced from meteor observations". *Medd. Lund Obs.*, Ser. I, **226**, 1029–1043.

Lindblad B.A. (1968). "Long-term variations in meteor radar rates, heights and radar-echo amplitudes". In Kresak L. and Millman P.M., editors, *Physics and Dynamics of Meteors, Proceedings of IAU Symposium 33*, Tatranská Lomnica, Czechoslovakia, Reidel Publishing Company, Dordrecht, Holland, pages 50–62.

Lindblad B.A. (1968c). "A long-term variation in mesophere, lower thermosphere density and its relation to the solar cycle". *Medd. Lund Obs.*, Ser. I, **237**, 835–844.

Lindblad B.A. (1969). Measurement of micrometeorites impacts from a sounding rocket during a noctilucent cloud display". *Medd. Lund Obs.*, Ser. I, **244**, 190–196.

Lindblad B.A. (1970). "Rocket observations of micrometeorites". *Medd. Lund Obs.*, Ser. I, **249**, 295–304.

Lindblad B.A. (1971a). "Meteor streams". *Medd. Lund Obs.*, Ser. I, **250**, 287–297.

Lindblad B.A. (1971b). "A study of asteroid families and streams by computer techniques". *Medd. Lund Obs.*, Ser. I, **252**, 337–353.

Lindblad B.A. (1971c). "A stream search among 865 precise photographic meteor orbits". *Smithson. Contr. Astrophys.*, **12**, 1–13.

Lindblad B.A. (1971d). "A computerized stream search among 2401 photographic meteor orbits". *Smithson. Contr. Astrophys.*, **12**, 14–24.

Lindblad B.A. (1972). "The system of short period meteor streams". In Cristescu C., Klepczynski W.J., Milet B., editors, *Asteroids, Comets and Meteoric matter, IAU Colloquium 22*, Nice, France, Editura Academiei Republicil Socialiste Romania, pages 269–282.

Cook A.F., Lindblad B.A., Marsden B.G., McCrosky R.E., and Posen A. (1973). "Yet another stream search among 2401 photographic meteors". *Smithson. Contr. Astrophys.*, **15**, 1–5.

Lindblad B.A. (1974). "The system of short period meteor streams". *Medd. Lund Obs.*, Ser. I, **254**, 269–281.

Lindblad B.A. (1976a). "Meteoroid densities". In Elsässer H and Fechtig H., editors, *Interplanetary Dust and Zodiacal Light*, Springer-Verlag, pages 373–378.

Lindblad B.A. (1976b). "Meteor radar rates and the solar cycle". In Elsässer H and Fechtig H., editors, *Interplanetary Dust and Zodiacal Light*, Springer-Verlag, page 390.

Štohl J., Lindblad B.A. (1977). "Discussion of magnitude errors and magnitude scales of meteor observers in Sweden and Czechoslovakia". *Bull. Astr. Inst. Csl.*, **28**, 321–328.

Lindblad B.A. (1980). "Serial correlation of meteor radar rates". In Halliday I. and McIntosh B.A., editors, *Solid Particles in the Solar System, Proceedings of IAU Symposium 90*, Ottawa, Canada, Reidel Publishing Company, Dordrecht, Holland, pages 105–108.

Lindblad B.A. and Simek M. (1983a). "Structure and activity of Perseid meteor stream from radar observations 1956–1978". In Lagerkvist C.I. and Rickman H., editors, *Asteroids, Comets, Meteors*, Uppsala, Sweden, Reprocentralen, Uppsala, pages 431–434.

Lindblad B.A. and Simek M. (1983b). "Errors in visual meteor observations". In Lagerkvist C.I. and Rickman H., editors, *Asteroids, Comets, Meteors*, Uppsala, Sweden, Reprocentralen, Uppsala, pages 451–455.

Lindblad B.A. (1986a). "Structure and activity of the Perseid meteor stream from visual observations". In Lagerkvist C.I. and Rickman H., editors, *Asteroids, Comets, Meteors II*, Uppsala, Sweden, Reprocentralen, Uppsala, pages 531–535.

Lindblad B.A. (1986b). "The activity curve of the Perseid meteor stream from Onsala radar observations". In Lagerkvist C.I. and Rickman H., editors, *Asteroids, Comets, Meteors II*, Uppsala, Sweden, Reprocentralen, Uppsala, pages 537–540.

Lindblad B.A. (1986c). "Spurious maxima and minima in meteor stream profiles". In Lagerkvist C.I. and Rickman H., editors, *Asteroids, Comets, Meteors II*, Uppsala, Sweden, Reprocentralen, Uppsala, pages 545–548.

Lindblad B.A. (1986d). "Meteor heights derived from radar-visual observations". In Lagerkvist C.I. and Rickman H., editors, *Asteroids, Comets, Meteors II*, Uppsala, Sweden, Reprocentralen, Uppsala, pages 615–620.

Lindblad B.A. (1987a). "The 1985 return of the Giacobinid meteor stream". In *ESA Proceedings of the 20th ESLAB Symposium on the Exploration of Halley's Comet. Volume 2: Dust and Nucleus*, pages 229–230.

Lindblad B.A. (1987b). "Comet 1944 I and the November Monocerotids". *WGN, Journal of the IMO*, **15**, 154.

Lindblad B.A. (1990). "The Orbit of the Eta Aquarid Meteor Stream". In Lagerkvist C.I., Rickman H. and Lindblad B.A., editors, *Asteroids, Comets, Meteors III*, Uppsala, Sweden, June 12–16, 1989, Uppsala, Uppsala Universitet, page 551.

Lindblad B. A. and Porubčan, V. (1991). "Activity and orbit of the Lyrid Meteor Stream" In *Abstracts for the International Conference on Asteroids, Comets, Meteors 1991.* Flagstaff, Arizona, page 137.

Lindblad B. A. and Porubčan, V. (1994). "The activity and orbit of the Perseid meteor stream". *Planetary and Space Science*, **42**, 117–122.

Lindblad B.A. (1998). "The nodal, the new and the old maximum of the Perseid meteor stream". *Planetary and Space Science*, **46**, 865–868.

Lindblad B.A. (2000). "A long-term high-resolution study of the visual activity curve of the Perseid meteor stream 1953–1983". *Planetary and Space Science*, **48**, 905–909.

Lindblad B.A. (2001). "Visible and radar observations of the Perseid meteor stream 1953–83". In Warmbein B., editor, *Proceedings of the Meteoroids 2001 Conference*, Kiruna, Sweden, ESA SP-495, Noordwijk, ESA Publications Division, pages 3–7.

Lindblad B.A. (2003). "Solar control of meteor radar rates" In Wilson A., editor, *Solar Variability as an Input to the Earth's Environment. International Solar Cycle Studies (ISCS) Symposium*, Tatranská Lomnica, Slovakia,ESA SP-535, Noordwijk, ESA Publications Division, pages 755–759.

Lindblad B.A., Neslušan L., Porubčan V., and Svoreň J. (2003). "IAU Meteor Database of photographic orbits version 2003". *Earth, Moon, and Planets*, **93**, 249–260.

Handling Editor: Marc Gyssens

Conferences

International Meteor Conference 2010 report

Vaibhav Savant [1]

Received 2010 October 9

This was my first international conference and as with all things that are first I was more than a little anxious as to how things would proceed. It all started about 5 years ago when we in Fergusson College, Pune, India started with Visual Observations of meteor showers. Even then skies around the city were bad and so observations were restricted only to the privileged few who could afford to spend time and resources to go away from city to less light polluted areas and stay away from work or studies for the period of the shower. I was introduced to the subject in late 2008 when I took my first visual observations along with my teacher – and now mother after having adopted me! – Dr. Ms. Raka Dabhade from a location away from Pune city's polluted skies. By this time we had already shifted to radio observations and had collected data using forward meteor scatter method for FM radio stations. But this had to be abandoned as more and more private FM radio stations started mushrooming and the radio shadow region was lost. After trying airband and failing miserably due to the low transmission power we decided to shift to ham radio observations. Also the frequencies were higher than required on airband. We simultaneously started with Photographic Observations. Using a DSLR with programmable timer release cord TC80N3 and self training and experimenting with the help of IMO's Handbook we were able to capture quite a few showers. Unfortunately the unpredictable weather in India started playing foul and now photographic observations can be taken intermittently only whenever weather allows.

At this point we got the opportunity to attend the International Meteor Conference 2010 at Armagh and what an experience it was! We missed the fireball workshop as our travel arrangements did not allow us to reach Armagh before mid noon. Registrations were done at the Youth Hostel where we were accommodated. We were pleasantly surprised to learn that mom and I had been put in the same room – many thanks to the organizers who lent a personal touch to the IMC 2010. The first evening was spent socializing at the Armagh Observatory and we were surprised to learn that delegates fromas many as 24 countries were present and that this was the first time India had participated. This was also the first time that after communicating with experts via emails that we finally met them in person and it also felt good to discuss with fellow hams who were present among the crowd as well. This came later though as the first evening was spent purely in getting to know who is who.

Figure 1 – OASES performance by local children and the Armagh Rhymers. Photo courtesy of Rafael Barrios.

Next day the opening of the conference was done by the Mayor of Armagh who welcomed all the delegates. The elaborate practical announcements by Apostolos Christou set an informal mood and instantly made us feel at home. After the invited talk on how NASA makes use of amateur meteor data for spacecraft operations I could not deny feeling a sense of pride. The topics scheduled were all intriguing as well as interesting and we could not wait to hear them out. I was particularly interested in the wide angle TV and the cheap all sky camera topics as these, I felt, could be implemented in our country. The meteor spectrum obtained by DSLR camera has inspired me to try out the method ourselves. I was glad our talk was slated in the first session as I could concentrate better on other topics after the presentation. After the first day's pro-

Figure 2 – The Conference is a great place for informal conversation. Here we see Prakash Atreya (FR), Jan Verbert (BE), Jeremie Vaubaillon (FR) and Nagatoshi Nogami (JP) talking. Photo courtesy of Bernd Brinkmann.

[1] Dept. of Instrumentation Science, University of Pune, India. Email: vaibhavsavant@gmail.com

IMO bibcode WGN-385-savant-imcreport
NASA-ADS bibcode 2010JIMO...38..142S

Figure 3 – IMC 2010 participants in front of the Market Place Theatre. Photo courtesy of Miruna Popescu.

gramme we were in very high spirits (only figuratively) as we realized there was so much that could be done be it with photographic, video or radio observations. Later in the evening we were treated with live Irish music by Armagh Rhymers at the Turner's Pub and after enjoying the social evening everyone was practically in high spirits!

In sessions 5 and 6, next day, we came to know of various trajectory determination methods developed and employed by meteor experts worldwide and the pros of using their own techniques as against cons of using others' techniques. I was specially impressed by the *optimal* all sky camera designed for amateurs and the HAM-Experiment which would allow scientists for the first time to see the behavior of a *known* meteor upon entering Earth's atmosphere. The participants were given a guided tour of the Armagh Observatory along with a very animated explanation of the Human Orrery. A visit to the Navan Center was next where everyone got a glimpse of the Navan culture as it existed in as early as 250 BC. The artifacts found there included pieces of pottery which date back to 4000 BC!

During dinner came the somber realization that it was our last evening together and I already started missing all the talks, all the friendships that were formed, all the good time we had had. But the astro poetry later with its songs, jokes and music perked everyone up and it was an evening full of fun and frolic. Last session was conducted next day and it was again a revelation with talks of how the moon which plays havoc with visual observations could be used to our advantage by observing impact flashes on the Moon during meteor showers. Lunch followed the closing sessions and group photograph after which we had to depart as the IMC 2010 at Armagh formally ended. We exchanged wishes with all the people we had met and with all the wonderful memories of the IMC which we would cherish for a long time started off for India. The IMC has been quite an experience for me thanks to all the organizers and participants who helped make it such a memorable one and I hope that you enjoyed reading as much as I did writing about it. Clear skies and meet you at the next IMC!

Handling Editor: Javor Kac

Figure 4 – Astropoetry show is one of the IMC traditions. Photo courtesy of the author.

Details of the Proceedings of IMC 2008, Šachtička, Slovakia

Communicated by Stanislav Kaniansky

Those who have attended an International Meteor Conference (IMC) will know that they present many high-quality papers on a wide range of meteor subjects. This material is less well known outside the circle of conference-goers, however. To make it more widely available, we are publishing a list of all IMC 2008 papers here.

Those who attended the Conference will already have the Proceedings. Others can order them from the IMO: details are in the lower half of the inside back cover of this Journal and on the IMO website.

IMO bibcode WGN-385-imc2008proc NASA-ADS bibcode 2010JIMO...38..144K

Ongoing meteor work

What is the difference between image intensifier and CCD meteors? III. How do meteor showers look like by image intensifiers and by CCD?

Masahiro Koseki [1], *Masayoshi Ueda* [2] *and Yoshihiko Shigeno* [3]

A limited number of major meteor showers, such as the Geminids and δ-Aquariids, could be observed well by each observational technique including photographic and radar observations. The properties of a meteor shower differ according to the observing technology. We compare two video observations, Shigeno's image intensifier observations and Ueda's CCD observations for the major showers and some other meteor sources.

Received 2010 March 20

1 Differences found in major showers

We applied intervals (Table 1) to list candidate meteors for each meteor shower or source from the following bases:

1. We take the mean orbital elements of the meteor showers mainly from Lindblad (1971).
2. We calculate the Southworth-Hawkins (1963) D-criterion $D_S(M, N)$ for all photographic meteors and select the meteors with $D_S < 0.25$ as candidates.
3. We define the search region from their outer limits.

Table 1 – Searched intervals for major meteor showers and ecliptic showers (source).

	$\lambda_\odot$	$\lambda - \lambda_\odot$	β
Perseids	115∼155	275∼295	+30∼+45
Geminids	240∼275	200∼215	0∼+20
Leonids	200∼265	260∼285	0∼+20
η-Aquariids	30∼65	285∼300	0∼+15
Orionids	185∼225	240∼255	−15∼0
δ-Aquariids	115∼145	200∼225	−20∼0
α-Capricornids	95∼155	165∼195	−10∼+25
Quadrantids	280∼290	260∼285	+60∼+70
ANT (Ecliptic sources)	—	175∼210	−15∼+10
N,S-Taurids	175∼245	175∼210	−15∼+10
Comae Berenicids	200∼310	230∼255	+10∼+30

These intervals are based on the D-criterion calculation introduced by Southworth and Hawkins (1963). They assumed $D_S < 0.20$ for their 360 samples and Lindblad (1971) defined that D_S should vary inversely as the fourth root of the sample size. The definition by Lindblad might work well if the observational errors are small and the intention of the researchers is to resolve meteor showers. Here, we used $D_S < 0.25$ to search for the candidates, because we do not intend to define a meteor shower but to compare the differences between the observational techniques. It is necessary to identify samples that might be classified 'erroneous' or classified formerly as 'doubtful'. These intervals work well and give very interesting results which are described below.

1.1 η-Aquariids

The η-Aquariids are the most active Southern meteor shower and a difficult object for Northern hemisphere observers. Japan is more favourably situated than Europe and many observations have been carried out at dawn. It is necessary to note that Shigeno and his colleagues operated during their expedition in Australia to get photographic data in 1989 (Shigeno et al., 1997). They obtained fourteen double station η-Aquariids, although only eight data are given in the Harvard list (McCrosky & Posen, 1961), and only one η-Aquariid allowed a high precision reduction.

Shigeno and Ueda observed the η-Aquariids from Japan and got nine image intensifier meteors and twenty two CCD records. The three sources, e.g. photo, image intensifier and CCD, coincide with each other (Figures 1 and 2). The η-Aquariids are the rather unusual case that the three observing techniques agree well.

We assume in our papers that the radiant point in $\lambda - \lambda_\odot$ and β coordinates can be kept constant with time. It means that the orbital plane of the meteoroids simply rotates around the axis of the ecliptic plane with time. This procedure is useful as a first approximation to allow for the radiant drift but it is obvious that the radiant distribution changes with time even in $(\lambda - \lambda_\odot, \beta)$ coordinates.

For the η-Aquariids, the radiant point in $\lambda - \lambda_\odot$ and β moves with time and the radiant point distribution seems to be elongated (Figure 2). The shift in $\lambda - \lambda_\odot$ and β with time is represented: $\lambda - \lambda_\odot = 293.^\circ76 - 0.220(\lambda_\odot - 45^\circ)$, $\beta = 7.^\circ50 + 0.062(\lambda_\odot - 45^\circ)$. This radiant drift corresponds to the equatorial coordinates as listed in Table 2.

[1] 4-3-5 Annnaka Annaka-shi, Gunma-ken, 379-0116, Japan. The Nippon Meteor Society (NMS)
Email: geh04301@nifty.ne.jp
[2] 43-2 Asuka Habikino-shi Osaka, 583-0842, Japan. The Nippon Meteor Society (NMS)
Email: ueda@meteor.chicappa.jp
[3] 5-6 Kizuki-Sumiyoshi, Kawasaki City, 211-0021, Japan. Meteor Science Seminar (MSS)
Email: cyg@nikon.co.jp

IMO bibcode WGN-385-koseki-ccd3
NASA-ADS bibcode 2010JIMO...38..145K

Table 2 – Radiant drift estimated from Japanese observations for the η-Aquariids.

$\lambda_\odot$	30	35	40	45	50	55	60	65	70
R.A.	327.0	330.6	334.1	337.6	341.0	344.5	347.9	351.4	354.8
Dec.	−6.3	−4.7	−3.0	−1.3	+0.4	+2.2	+4.0	+5.8	+7.6

The perihelion distribution of the η-Aquariids is shown in Figure 3 with the Orionids and 1P/Halley. The argument of perihelion also changes with time while the perihelion distribution in ecliptic coordinates seems to remain constant. The perihelion distribution seems to be elongated too but this might be due to uncertainties in V_g (see next section). It is clear that the perihelia of the η-Aquariid meteoroids are distributed in the plane of the orbit of 1P/Halley.

1.2 Orionids

The Orionids represent one of the best observable meteor showers in Japan because the radiant passes near the zenith and its long activity begins when the rainy autumn season has ended in most parts of Japan. Both image intensifier and CCD techniques recorded Orionid meteors. We studied and compared the Orionid meteor images by both methods (Figures 7 and 8 in Koseki, Ueda & Shigeno 2010a). It is clear that the recorded trails are short and difficult objects for calculating meteor orbits exactly.

Figures 7 and 5 show the geocentric velocity distribution along the time of the observations ($\lambda_\odot$). The initial data interval for the Orionids seems to be biased towards the earlier dates and the Orionid activity may continue longer and later than the supposed period. The conventional meteor shower surveys use the Southworth-Hawkins D-criterion but this is based on the assumption that the meteoroid distribution is symmetrical about the core of the stream. Ordinary meteor streams are asymmetrical and therefore it is necessary to search carefully the outskirts of the activity by investigating the individual radiant points and the velocity.

The observed velocity distribution by CCD includes some slower meteors but they are neither sporadics nor related to a new shower. The sporadic activity in this area seems to be low in image intensifier observations and all image intensifier meteors are fast. It is very likely that the short Orionids in the vicinity of the radiant do not yield enough information on the meteor trail. The dispersion in the velocity determination affects the dispersion in the argument of perihelion (Figure 8).

Image intensifier and CCD observations give a similar picture for the radiant distributions: elongated to the right and left with a small contamination from sporadics (Figures 4 and 6). This shape is caused by the radiant drift with time and does not show any original radiant structure. The radiant drift as a function of time suggests that the radiants belong to one continuous activity. The radiant moves in $(\lambda - \lambda_\odot,\ \beta)$ coordinates: $\lambda - \lambda_\odot = 246\overset{\circ}{.}82 - 0.199(\lambda_\odot - 210°)$, $\beta = -7\overset{\circ}{.}72 + 0.070(\lambda_\odot - 210°)$. This radiant shift corresponds to the equatorial coordinates as listed in Table 3.

Table 3 – The Orionids radiant point drift from CCD observations.

$\lambda_\odot$	200	205	210	215	220	225
R.A.	88.8	92.9	97.0	101.2	105.3	109.4
Dec.	+15.0	+15.3	+15.6	+15.6	+15.6	+15.5

Image intensifier observations during the Orionid maximum suggest that the radiant itself is not a point but an ellipse. The radiant distribution from image intensifier data (Figure 6), split into two classes of mean velocity, shows that the east-westward spread might be unrelated to the difference in velocity. It is possible that the radiant shape during the maximum is caused by orbital spread but we do not study the details of it here. The disperson in velocity influences very much the

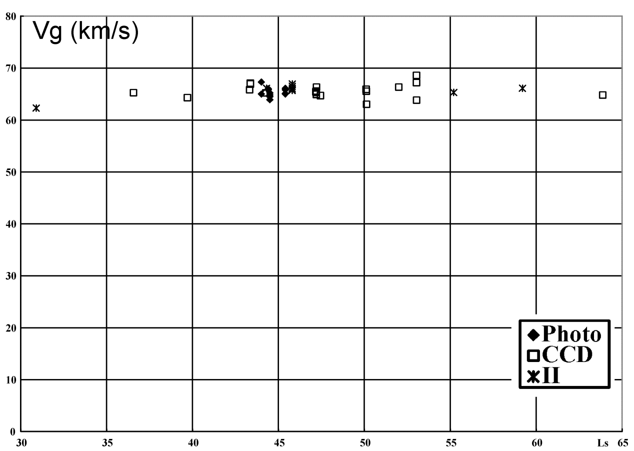

Figure 1 – Geocentric velocity distribution of the η-Aquariid meteors observed by Japanese observers.

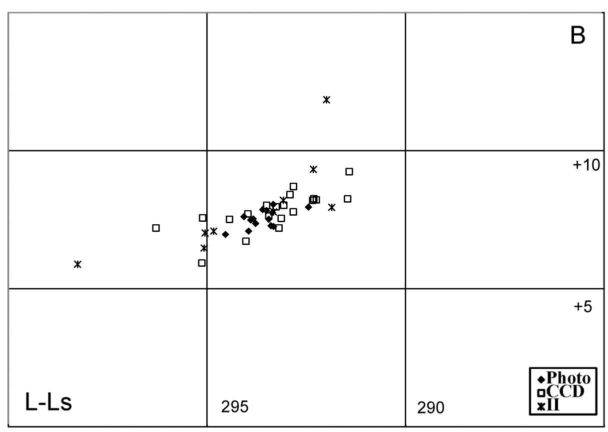

Figure 2 – η-Aquariid radiant point distribution in $(\lambda - \lambda_\odot,\ \beta)$ coordinates.

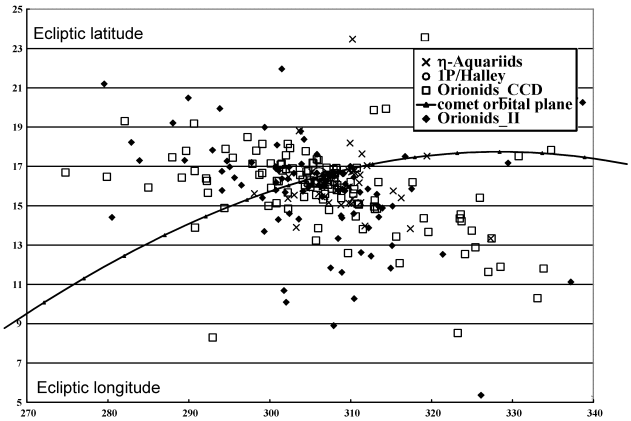

Figure 3 – The perihelion distributions of the η-Aquariids and Orionids in the ecliptic coordinates.

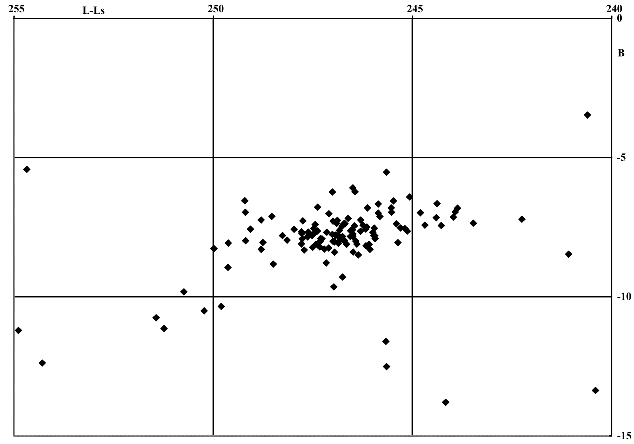

Figure 4 – Radiant distribution of CCD Orionids.

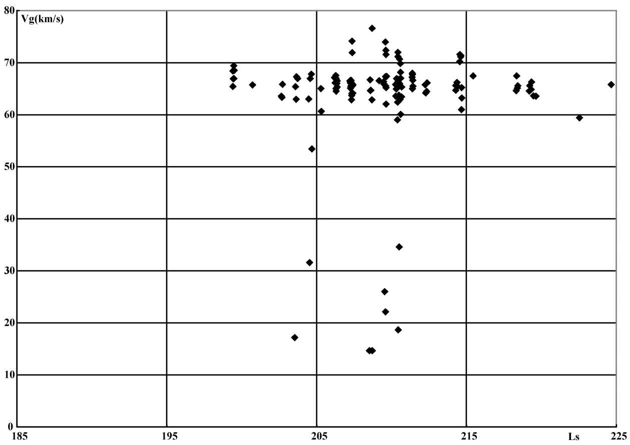

Figure 5 – Geocentric velocity distribution of Orionid meteors observed by CCD.

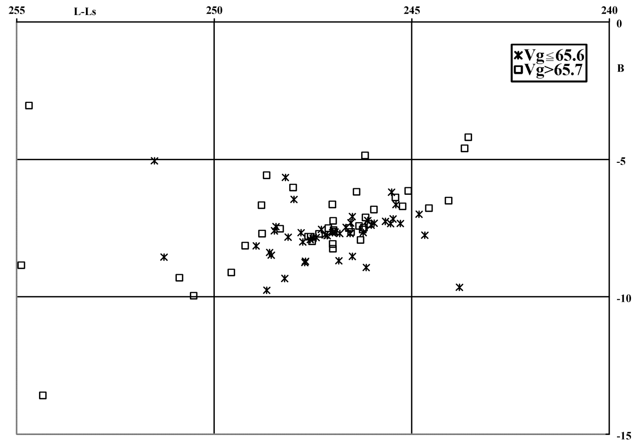

Figure 6 – Radiant distribution of image intensifier Orionids in two velocity ranges.

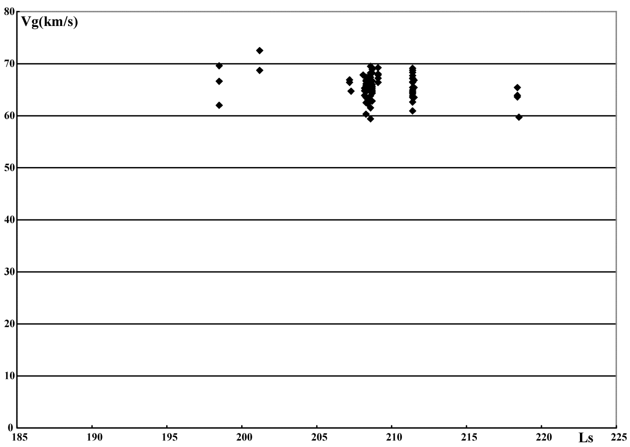

Figure 7 – Geocentric velocity distribution of Orionid meteors observed by image intensifiers.

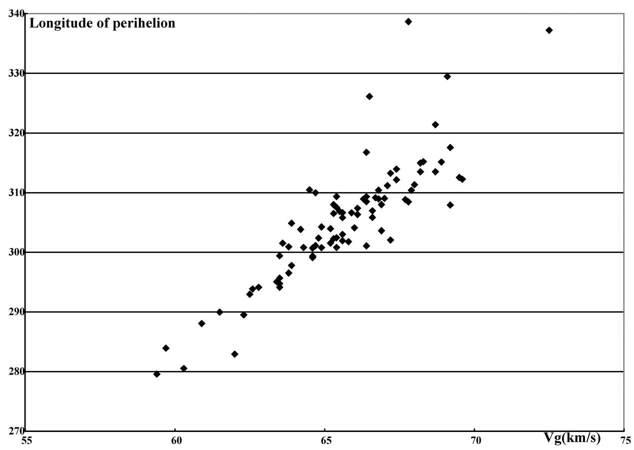

Figure 8 – The perihelion longitude and observed velocity dispersion of Orionid meteors from image intensifiers.

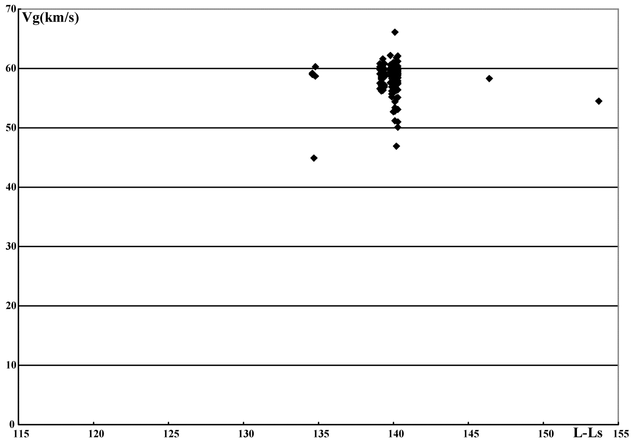

Figure 9 – Geocentric velocity distribution of the Perseid meteors observed by image intensifier.

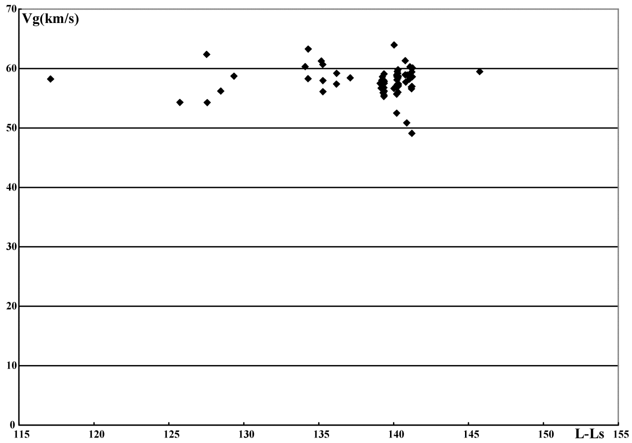

Figure 10 – Geocentric velocity distribution of the Perseid meteors observed by CCD.

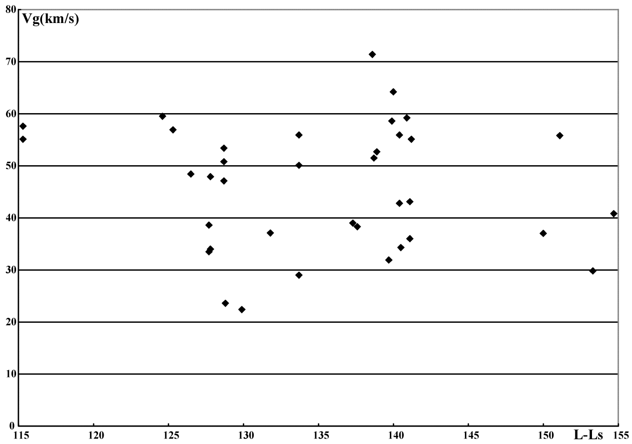

Figure 11 – Geocentric velocity distribution of the Perseid meteors observed by radar (Harvard 1961–65).

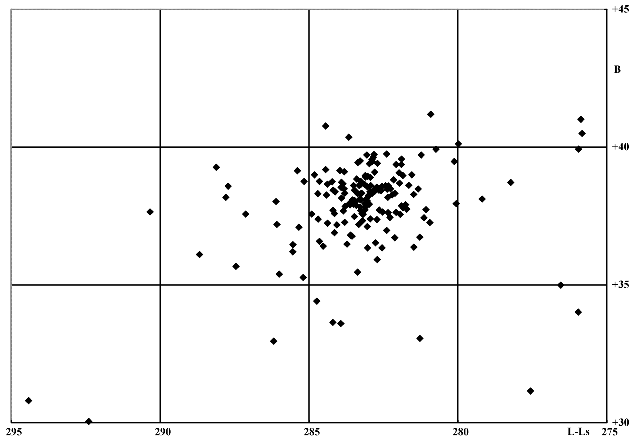

Figure 12 – Radiant distribution of image intensifier Perseids.

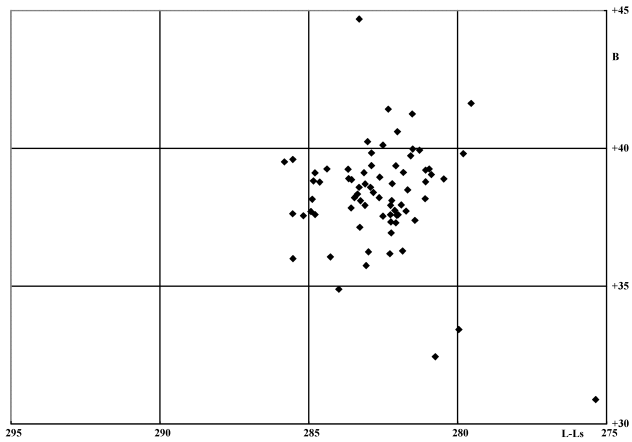

Figure 13 – Radiant distribution of CCD Perseids.

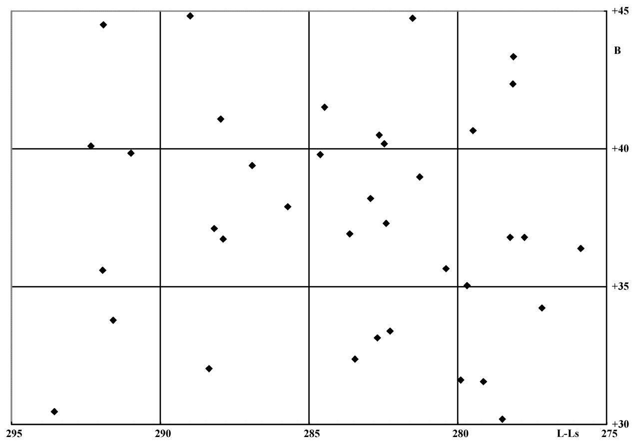

Figure 14 – Radiant distribution of radar Perseids (Harvard 1961–65).

Table 4 – Comparison of observed magnitude distributions by image intensifiers.

	1993 August 12/13		1993 October 24/25	
Magnitude	Perseids	Sporadics	Orionids	Sporadics
−6	1	0	0	0
−5	0	0	0	0
−4	2	1	0	0
−3	1	0	0	0
−2	2	0	2	1
−1	1	0	1	0
0	5	0	0	0
1	12	0	1	1
2	29	2	2	3
3	16	6	4	6
4	28	11	4	8
5	50	16	18	20
6	23	8	13	12
Total	170	44	45	51
Mean	3.51	4.32	4.36	4.45

uncertainties in the orbit especially in the argument of perihelion. It is not clear which orbital structure causes the radiant ellipse in view of the velocity uncertainty. The distribution of the perihelion shows an interesting shape that elongates from 1P/Halley and might overlap with η-Aquariids (Figure 3). The spread of Orionids and η-Aquariids requires further research to determine if this is relevant or not.

1.3 Perseids

The Perseids are the most active meteor shower year by year for many observational techniques except for radar. Their magnitude distributions show that the Perseids are richer in bright meteors than the Orionids (Table 4).

The Perseids seem to be weak in faint meteors or to be a difficult object for radar observations. Figures 9 to 14 show this situation clearly and suggest that CCD and image intensifier observations are situated between photography and radar techniques. Image intensifiers can record fainter meteors than CCD (Koseki et al., 2010b). The mean magnitude of the Perseids is smaller than for sporadics and the contribution from sporadics in the fainter meteor population is predominant over the Perseids. Radiant distributions of Perseids by image intensifiers (Figure 12) and by radar (Figure 14) are much contaminated by sporadics and it is impossible to define the center of the radiant in the radar radiant distribution. This is the very reason for the overestimation of the error in geocentric velocity for both the image intensifier and radar data sets (Figures 11 and 13 in Koseki et al., 2010a). The practical error estimate could not be adapted to the more sensitive observations, especially for radar (Koseki et al., 2010a). These are affected by sporadic contamination and have the possibility to detect the outskirts of a stream. Obviously the effect of sporadics on image intensifier meteors is stronger than for CCD meteors and, therefore, the practical error in geocentric velocity of image intensifier meteors might be a little bit smaller than for CCD meteors.

Table 5 – Radiant drift estimated from the CCD observations for Perseids.

$\lambda_\odot$	115	120	125	130	135	140	145	150
R.A.	14.6	20.5	26.7	33.3	40.3	47.7	55.4	63.5
Dec.	50.0	51.8	53.5	55.0	56.4	57.7	58.7	59.5

The Perseid radiant seems to be stationary in ($\lambda - \lambda_\odot$, β) coordinates. But when we adopted the least squares solution for the CCD observations, we would get $\lambda - \lambda_\odot = 281\overset{\circ}{.}75 + 0.065(\lambda_\odot - 125°)$, $\beta = 39\overset{\circ}{.}10 - 0.062(\lambda_\odot - 125°)$ and the corresponding radiant drift in equatorial coordinates (see Table 5).

The perihelia of image intensifier and CCD Perseids are distributed along the orbital plane of 109P/Swift-Tuttle (Figure 15). Unlike the Orionid distribution, this scheme seems to be real, because the argument of perihelion is not influenced by the uncertainty of the observed velocity.

1.4 Geminids

The Geminids are the best recorded meteor shower by all observations because of their medium speed and the fact that the shower is rich in faint meteors. This shower

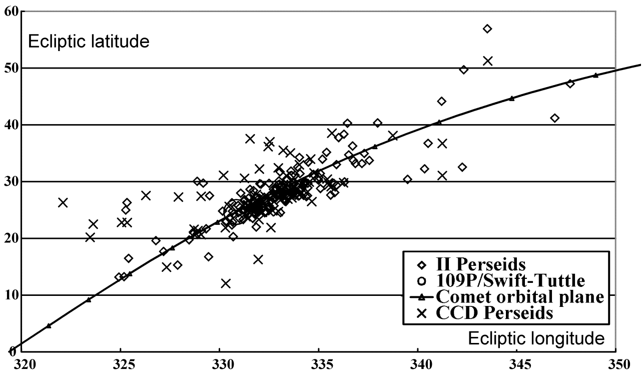

Figure 15 – The perihelion distributions of the Perseids in ecliptic coordinates.

Table 6 – Assumed practical errors in meteor velocity determinations for Geminids. Photographic observations are divided into G (graphical reduction), P (precise reduction), C (Czechoslovakia results) and S (Soviet results), and the radar observations into 61–65 (Harvard 1961–65) and 68–69 (Harvard 1968–69) each.

	CCD	II	G	P	C	S	61–65	68–69
Mean	32.6	33.1	34.9	34.4	35.5	35.2	35.8	35.4
S.D.	1.25	2.55	1.83	0.48	0.71	2.41	3.84	5.33

is the most suitable case to compare the difference between the observational techniques.

The practical error in geocentric velocity of radar meteors could be estimated using Geminids, because the sporadic contamination effect is smaller than for any other shower (Table 6).

The standard deviations for the radar observations are still larger than for the photographic data but the contamination by sporadics is important even for the Geminids (Figures 16, 17, 18 and 19). The standard deviation for the image intensifier data is larger than for the CCD data, but the contamination is less. Can image intensifiers not observe meteors precisely? No, image intensifiers and radar can record fainter meteors than CCD and photographic techniques. This may indicate that the spread in velocity and in the orbit itself becomes larger with decreasing meteoroid mass.

The comparison of the radiant distributions for different observing techniques reveals another aspect of the Geminid stream structure. Each observing method shows an elliptical radiant shape (Figures 16, 17 and 18) because the Geminid radiant shifts in $(\lambda - \lambda_{\odot}, \beta)$ coordinates. The radiant moves along the major axis of the ellipse and Ueda's CCD observations result in $\lambda - \lambda_{\odot} = 209.^{\circ}89 - 0.154(\lambda_{\odot} - 250^{\circ})$, $\beta = 10.^{\circ}60 - 0.009(\lambda_{\odot} - 250^{\circ})$. We can transfer the radiant point shift into equatorial coordinates (Table 7).

But this is not the exact reason for the elliptical shape of the Geminid radiant. Shigeno's observations (Figure 16) have been done mainly around the time of the maximum and do not include the outskirts of the activity period. The elliptical shape cannot be explained by the radiant drift with time but is caused by its orbital structure.

Each observing technique shows the same elliptical shape for the radiant but the ellipse becomes larger for fainter meteors, which means that the radar and image intensifier radiants are more dispersed. The Geminid meteoroids are diffused at perihelion mainly in the orbital plane and in inclination according to the dispersion in the perihelion. The smaller the meteoroid, the wider the spread becomes.

The perihelion coordinates of the Geminid meteoroids are spread across the orbital plane of its supposed parent body 3200 Phaethon and, therefore, their inclinations are diffused (Figure 19). The left side of the radiant point ellipse, which is the east side, is the equivalent to the left part of the perihelion distribution. The perihelion tends to shift from the upper left to the lower right during the activity.

1.5 Leonids

The Leonids are one of the most impressive 'periodic showers' and Shigeno recorded the great storm in 2001 by image intensifier. However, the recorded numbers were rather small although visual observers reported hourly rates of several hundreds. Koseki got magnitude distributions by image intensifier for the Leonids and the Giacobinids for the 1998 apparitions (Table 9). Apparently the Leonids are rich in bright meteors but poor in faint meteors although in 2002 Ueda observed faint Leonids, mainly under +4th magnitude, by video observations.

The 2001 Leonid radiant distribution by image intensifier is very concentrated while for the other years it is remarkably diffuse in contrast to 2001 (Figure 20). Radar observations in 1961–65 show a very similar distribution although they covered the previous Leonid return (Figure 22). The Leonid radiant is situated near the apex and the more sensitive devices are significantly affected by sporadics from the apex source.

CCD Leonid radiants for 2004–05 show a rather diffuse distribution and are supposed to be typical for the poor activity period (Figure 21). The velocity distribution from CCD data suggests a prolonged activity of the Leonids in spite of the low activity period (Figure 23). We selected radiants located within the range of $270 \leq \lambda_{\odot} < 276$ and $+8 \leq \beta < +13$ to belong to the 'core' and others to belong to the 'mantle'. The so-called 'mantle'-Leonid activity continues longer than that of the 'core'-Leonids. There may be some contaminations from the apex source except for the maximum period but the Orionid activity suggests a shower of retrograde motion can be active for longer than previously supposed. It is necessary to study the possibility whether such retrograde showers could contain meteoroids drifting away and expanding like 'ecliptic showers'.

The Leonid radiant also moves along $\lambda - \lambda_{\odot} = 276.^{\circ}00 - 0.321(\lambda_{\odot} - 225^{\circ})$, $\beta = +11.^{\circ}41 - 0.103(\lambda_{\odot} - 225^{\circ})$ and can be represented in equatorial coordinates as Table 8.

Table 7 – Radiant drift estimated from CCD observations for the Geminids.

$\lambda_{\odot}$	245	250	255	260	265	270
R.A.	96.7	101.7	106.7	111.6	116.4	121.2
Dec.	+34.0	+33.6	+33.2	+32.6	+31.9	+31.0

Table 8 – Leonid radiant point drift estimated from CCD observations.

$\lambda_{\odot}$	220	225	230	235	240	245
R.A.	144.1	147.4	150.6	153.8	156.9	160.0
Dec.	+26.9	+25.3	+23.6	+22.0	+20.2	+18.5

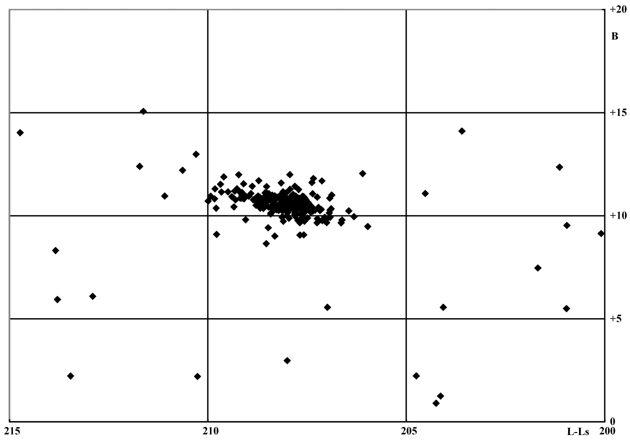

Figure 16 – Radiant distribution for image intensifier Geminids.

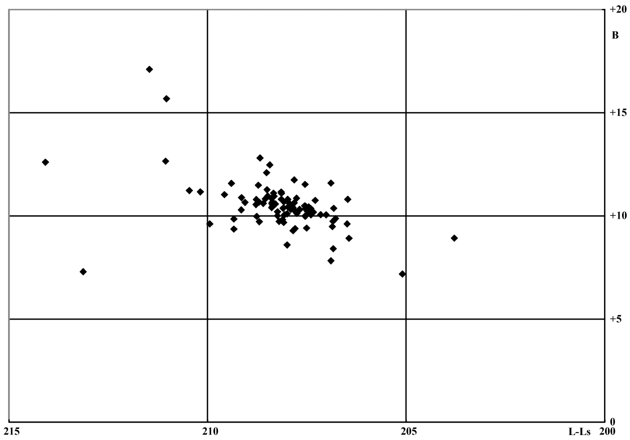

Figure 17 – Radiant distribution for CCD Geminids.

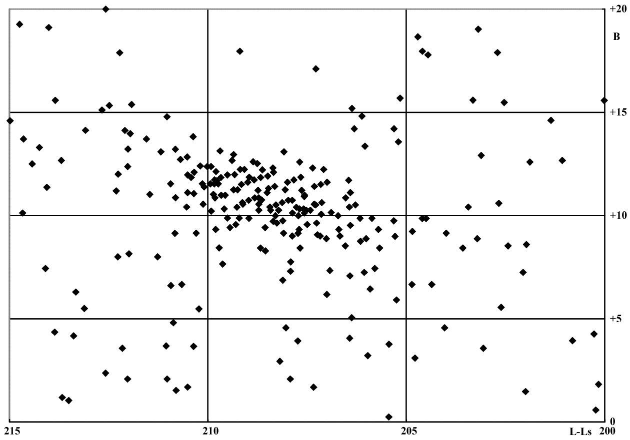

Figure 18 – Radiant distribution for radar Geminids (Harvard 1961–65).

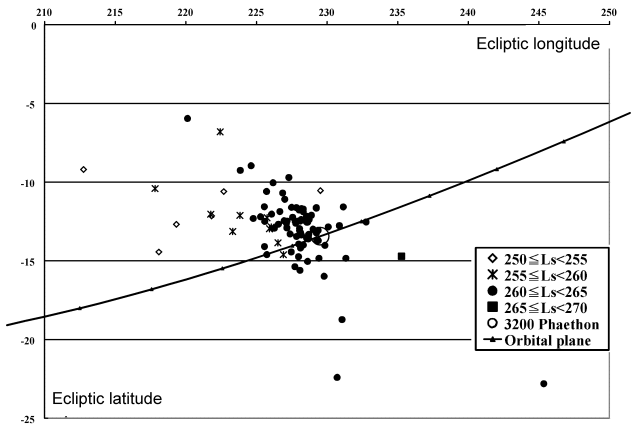

Figure 19 – The perihelion distributions for Geminids in ecliptic coordinates.

Table 9 – Magnitude distributions of the 1998 Giacobinids and 1998 Leonids by image intensifier.

	1998 October 8/9		1998 November 17/18	
Magnitude	Giacobinids	Sporadics	Leonids	Sporadics
−4	0	0	1	0
−3	0	0	1	0
−2	2	0	3	0
−1	1	0	0	0
0	1	0	2	0
1	5	0	2	1
2	14	4	4	1
3	29	8	1	1
4	49	9	8	2
5	51	20	7	11
6	23	5	5	18
Total	175	46	34	34
Mean	4.02	4.3	2.85	5.21

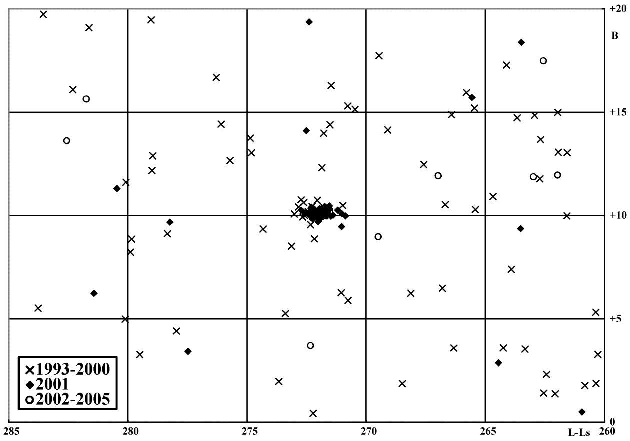

Figure 20 – Radiant distribution of image intensifier Leonids showing the concentrated radiant for the high activity in 2001.

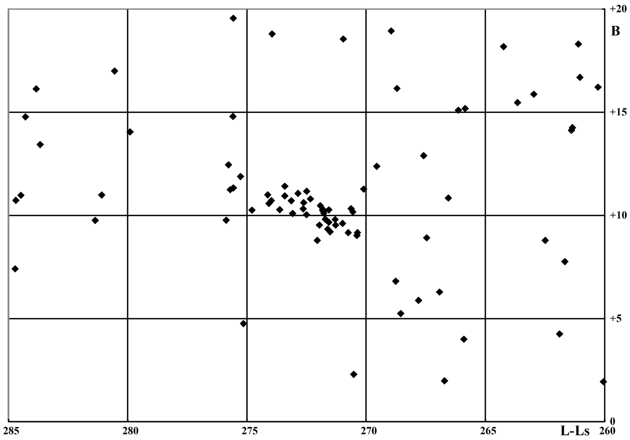

Figure 21 – The radiant distribution of CCD Leonids.

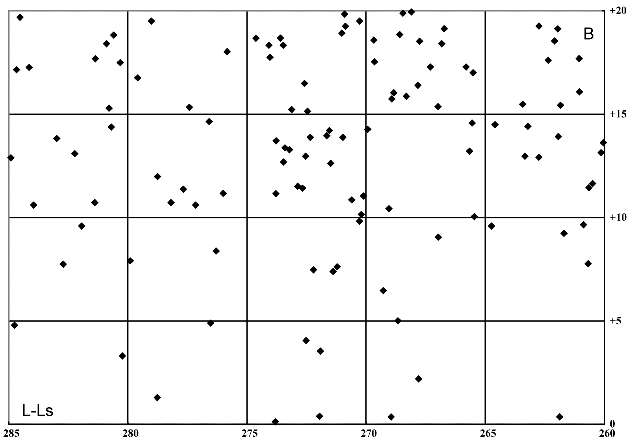

Figure 22 – Radiant distribution for radar Leonids (Harvard 1961–65).

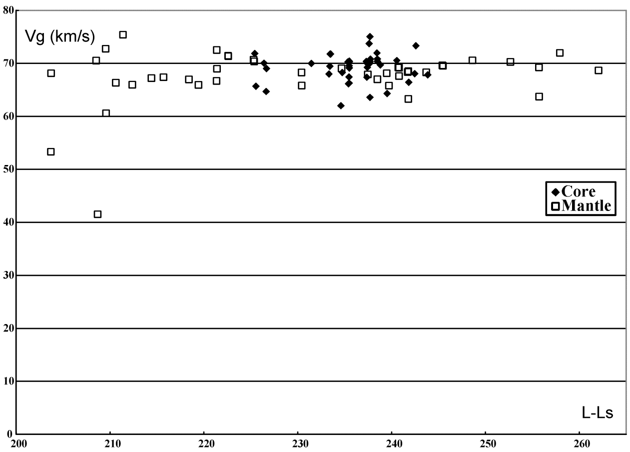

Figure 23 – Comparing the geocentric velocity distribution of the Leonid meteors observed by CCD for the core with the mantle.

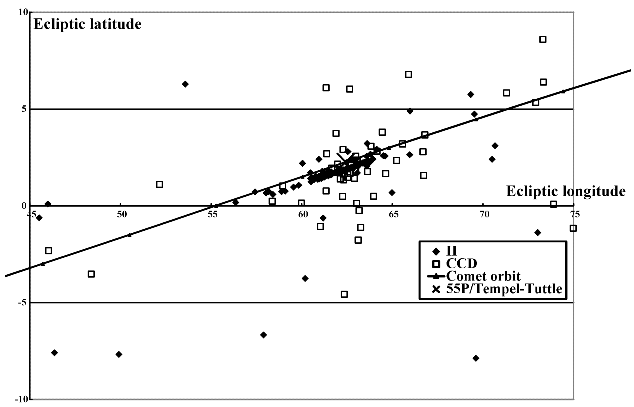

Figure 24 – The perihelion distribution for the Leonids in ecliptic coordinates.

The perihelia of image intensifier and CCD Leonids are distributed along the orbital plane of 55P/Tempel-Tuttle (Figure 24). This scheme is similar to the Perseids but different from the Geminids and the Orionids.

1.6 δ-Aquariids

The δ-Aquariids have been well observed by all observational methods from visual to radar and the results from all the observing techniques are in good agreement.

The magnitude distributions and the geocentric velocity determine what we can see by different observational methods. The Orionid magnitude distributions (Table 4) compare better to the sporadic magnitude distributions than that of the δ-Aquariids (see Table 11), and a population richer in fainter meteors is assumed to be more suitable for radar techniques. However, although the δ-Aquariids are less abundant in faint meteors they still have many faint meteors while their slower velocity is more suitable for radar work than the high velocity of the Orionids.

There is a small difference between the observing techniques for the δ-Aquariids as the proportion of shower members to sporadics decreases with the sensitivity of the technique. CCD observations are less affected by sporadics than image intensifier data although the proportion is larger than for other showers, except for the Geminids.

Shigeno (2004) reported the results of his group's expeditions to Australia. They had carried out two expeditions, the first in July 1998 and the second in August 2002, and they obtained an abundant number of Southern-δ-Aquariids. The results are in excellent agreement with earlier studies.

Shigeno's expedition to Australia suggested that the magnitude distribution of the δ-Aquariids compares very well with the sporadic magnitude distribution (see Table 11). Here, we considered meteors radiating from the area $205 \leq \lambda - \lambda_\odot < 215$ and $-15 \leq \beta < -5$ as δ-Aquariids and all others as sporadics, except for the α-Capricornids (see Section 2.2 α-Capricornids).

It is noteworthy to mention that the radiant distribution between the δ-Aquariids and the α-Capricornids does not indicate any distinct meteor shower activity (Figure 25). Both the Piscis Australids and ι-Aquariids could not be detected by Southern hemisphere image intensifier observations.

The radiant point moves in $(\lambda - \lambda_\odot, \beta)$ coordinates and we can determine the following relationship from the image intensifier meteors for which $204 \leq \lambda - \lambda_\odot < 215$, $-13 \leq \beta < -4$: $\lambda - \lambda_\odot = 210\overset{\circ}{.}99 - 0.232(\lambda_\odot - 120^\circ)$, $\beta = -7\overset{\circ}{.}19 - 0.056(\lambda_\odot - 120^\circ)$. This corresponds to the equatorial drift shown in Table 10.

Table 10 – Radiant point drift of the δ-Aquariids estimated from image intensifier observations in Australia.

$\lambda_\odot$	120	125	130	135	140	145
R.A.	335.7	339.5	343.3	347.0	350.7	354.4
Dec.	−17.8	−16.7	−15.5	−14.3	−13.0	−11.8

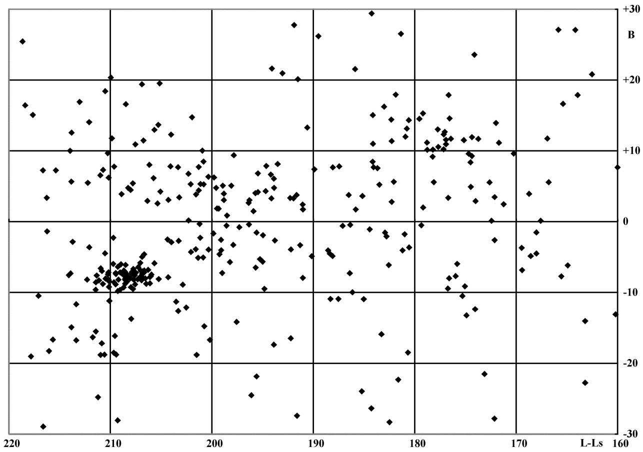

Figure 25 – Radiant distribution near the ANT area observed by image intensifier during the Australian expedition.

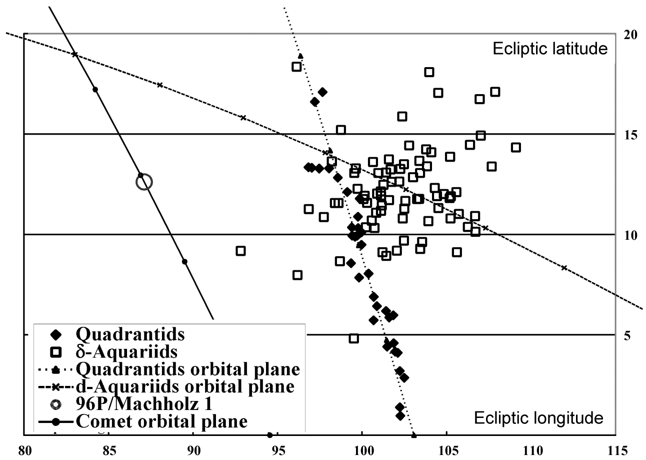

Figure 26 – Perihelion distribution for the Quadrantids and the δ-Aquariids from image intensifiers during the Australian expedition.

1.7 Quadrantids

It is not a surprise that Ueda missed the Quadrantids, because he did not observe in January 2004 and he could not observe in 2005 due to the unfavourable weather conditions. If we get no clear sky at the time of the maximum of this shower, we can record only a few Quadrantid meteors, which are not enough to determine the meteor activity. Photographic data were only recorded in 1954 and the Harvard radar observations of 1968–69 include no Quadrantids at all.

Shigeno observed the Quadrantids in 1996 and 1997. His 1997 observations are valuable, because they cover the descending branch of activity missed by photographic and radar techniques. The mean magnitude for all Quadrantids by image intensifier was 2.8 and this may indicate that the Quadrantids are richer in bright meteors after the maximum than before, with mean magnitudes of 3.2 before and 2.3 afterwards respectively. The 1997 observations are closer to the maximum when brighter meteors may be abundant. The Quadrantids seem to be rich in bright meteors. Anyway, it is very important to note that a short duration meteor shower could not be detected by all observational techniques.

Table 11 – Comparison of magnitude distributions by image intensifier from Shigeno's expeditions to Australia.

	Sporadics		δ-Aquariids		α-Capricornids	
Magnitude	Number	Proportion	Number	Proportion	Number	Proportion
$-1\sim0$	1	0.3	1	1.3	1	2.8
$0\sim1$	4	1.1	3	3.8	0	0.0
$1\sim2$	8	2.1	4	5.0	0	0.0
$2\sim3$	13	3.5	8	10.0	1	2.8
$3\sim4$	44	11.7	8	10.0	0	0.0
$4\sim5$	89	23.7	33	41.3	9	25.0
$5\sim6$	161	42.8	21	26.3	21	58.3
$6\sim7$	54	14.4	2	2.5	4	11.1
$7\sim8$	2	0.5	0	0.0	0	0.0
Total	376		80		36	
Mean Mag.	4.96		4.20		5.19	

Figure 26 shows the perihelion distributions of the Quadrantids and the δ-Aquariids by image intensifier during the Australian expedition. It is assumed that the Quadrantids may be associated with 96P/Machholz 1 and that they are related to the δ-Aquariids. Both perihelia of the meteor showers are far from that of the comet. The Quadrantid perihelia are distributed parallel to the comet orbit and the δ-Aquariids perihelia spread towards them.

2 Ecliptic sources (Antihelion sources)

The so-called antihelion source is not as exact as its name because it is located slightly east from the exact antihelion point. They have been called ecliptic sources (or showers) for a long time which is relevant to identify their origin. A short period comet (Jupiter's family) which produces a meteoroid stream with a low inclination will be visible as a meteor shower radiating from near the antihelion point when it crosses the Earth's orbit. Such a meteor shower disperses soon and vanishes into the sporadic background. Many small particles revolve around the Sun in the ecliptic plane along elliptical orbits and they cause ecliptic radiant points located about ten to twenty degrees east of the antihelion point. We will investigate such ecliptic sources below and select the meteors with $175 \leq \lambda - \lambda_{\odot} < 210$ and $-15 \leq \beta < +10$ as ecliptic candidates.

We can observe different stages and have difficulties to distinguish an ecliptic meteor shower from the sporadic background. However the difficulty depends strongly on the observational techniques. Photographic and CCD observations can catch only bright meteors produced by larger particles which might be less perturbed than the smaller ones. An ecliptic source will look younger and more condensed by photo and by CCD than by radar.

Figures 17 and 18 of Koseki et al. (2010a) illustrate the difference between photo and radar observations. The radar radiants are distributed with a distinct tendency towards the north-east while the photographic radiants seem to have some distinct concentrations, Geminids; upper-left (north-east), δ-Aquariids; lower-left (south-east), α-Capricornids; upper-right (north-west) and Taurids (center). Figures 13 and 14 of Koseki et al. (2010a) show another aspect of the difference in geocentric velocity distribution with solar longitude. Photographic observations were carried out during almost the whole year while the radar observations were often interrupted. Therefore it is better to use photographic data rather than the radar in order to look for fluctuations in the ecliptic activities over the year. We can easily distinguish some showers in the velocity distribution, such as the Geminids, δ-Aquariids, α-Capricornids, Taurids and some others (Figure 14 in Koseki et al., 2010a).

Comparing CCD with image intensifier observations (Figure 16 and Figure 15 respectively in Koseki et al., 2010a), showed that the radiant distributions for CCD are similar to those from photographic data and the radiant distributions for image intensifiers are comparable with radar radiant distributions. We can derive the above-mentioned showers easily from the CCD radiant distribution. The Geminids and δ-Aquariids are dominant in the image intensifier radiants although no distinct concentration for the Taurids or the α-Capricornids appears. Although the image intensifier radiant distribution seems to be similar to the CCD radiant distribution, we should be cautious before concluding that image intensifier observations are equivalent to CCD observations. It is worthwhile to note that CCD observations have been carried out throughout the year, each night when the sky was clear, but image intensifier observations were only possible during a few nights a year due to its operational requirements (Koseki et al., 2010a). Image intensifier observations were done at many occasions during the activity period of the δ-Aquariids and the Geminids. It is suggested that the radiant distribution for the image intensifiers is more like that of the radar observations than suggested by the figure.

The ratio of the shower meteors / sporadic background differs widely from one observational technique to the other. We cannot treat ecliptic showers as one and only ANT on the basis of radar radiant distributions. CCD observations can pursue long and bright meteor activity and can distinguish some ecliptic show-

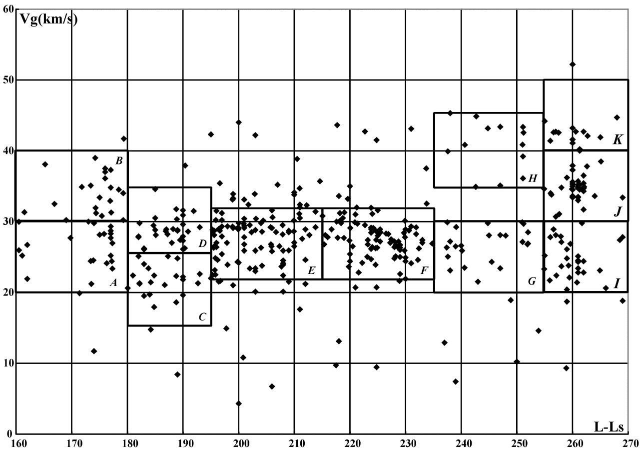

Figure 27 – Geocentric velocity distribution for photographic meteors for the Solar longitude interval 160 to 270 degrees.

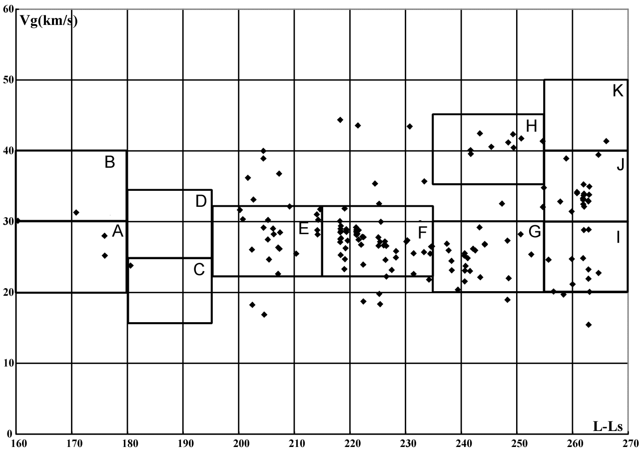

Figure 28 – Geocentric velocity distribution for CCD meteors for the Solar longitude interval 160 to 270 degrees.

Table 12 – Possible meteor activity during the Solar longitude interval 160–270 in the area of $175 \leq \lambda_\odot < 210$, $-15 \leq \beta < +10$.

Group A	$160 \leq \lambda_\odot < 180$	$20 \leq V_g < 30$
Group B	$160 \leq \lambda_\odot < 180$	$30 \leq V_g < 40$
Group C	$180 \leq \lambda_\odot < 195$	$15 \leq V_g < 25$
Group D	$180 \leq \lambda_\odot < 195$	$25 \leq V_g < 35$
Group E	$195 \leq \lambda_\odot < 215$	$22 \leq V_g < 32$
Group F	$215 \leq \lambda_\odot < 235$	$22 \leq V_g < 32$
Group G	$235 \leq \lambda_\odot < 255$	$20 \leq V_g < 30$
Group H	$235 \leq \lambda_\odot < 255$	$35 \leq V_g < 46$
Group I	$255 \leq \lambda_\odot < 270$	$20 \leq V_g < 30$
Group J	$255 \leq \lambda_\odot < 270$	$30 \leq V_g < 40$
Group K	$255 \leq \lambda_\odot < 270$	$40 \leq V_g < 50$

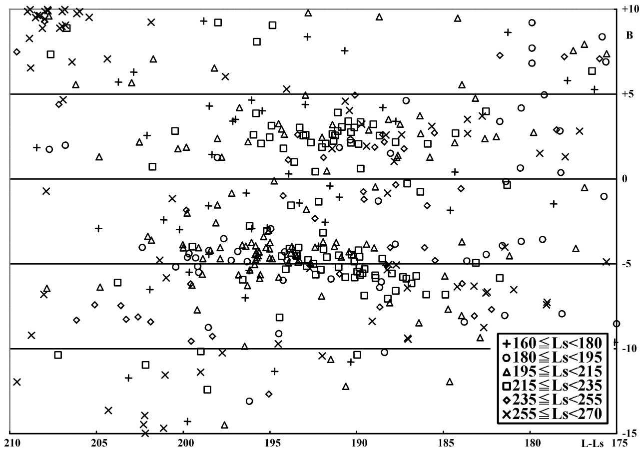

Figure 29 – Radiant distribution near the ANT area from photographic observations during the Solar longitude interval 160 to 270 degrees.

ers from the sporadic background. There is no need to make exceptions for the Taurids and the α-Capricornids. There are no distinct limits in both showers compared to sporadics (see below). We have doubts about their unity as they consist of several components. We will compare the details for image intensifier and CCD observations for both the Taurids and the α-Capricornids.

2.1 Taurids

Ecliptic sources are rich in brighter meteors and it is better to use photographic data in the first place to study the Taurids. Figure 27 shows the distribution of the geocentric velocity of the photographic ecliptic meteors along solar longitude $160 \leq \lambda_\odot < 270$. We can distinguish several concentrations from the sporadic background activity such as A∼K in this figure (Table 12). CCD observations display a similar distribution (Figure 28).

Figure 29 shows the photographic radiant distribution in this period divided into six sub-periods corresponding with the groups. It is clear that group J is the outskirts of the Geminids, K represents the December α-Monocerotids and H may be an unknown shower and they are not related to the Taurids. Groups D, E and F correspond to the Taurids and group I may be connected to the Taurids by a weak link with group G. Groups A, B and C are increments of sporadic activity and do not have any radiant concentrations.

It is very impressive that the Taurids show two components, the so-called Northern and Southern branches. They are located asymmetrically about the ecliptic plane and their activity periods do not coincide with

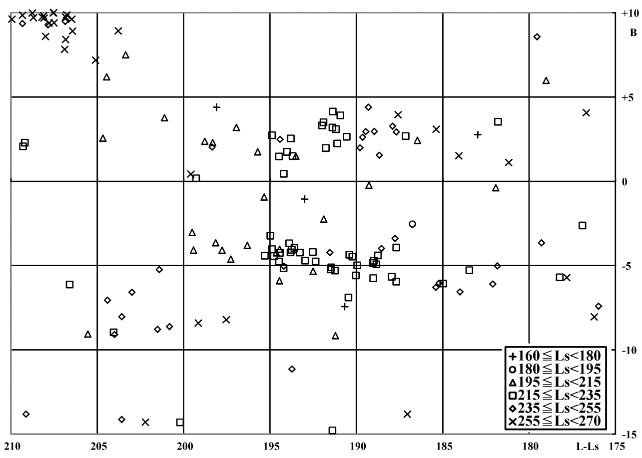

Figure 30 – Radiant distribution near the ANT area observed by CCD during the Solar longitude interval 160 to 270 degrees.

each other. However it is said that they share a common origin. Many hypotheses are possible because of the uncertainties in the basic scenario of the 'Taurids'. It is necessary to determine the statistical significance of the Taurids not only by photography but also by image intensifiers and CCD.

Neither image intensifier nor radar observations are useful to define activity profiles because of their observational restrictions (Koseki et al., 2010a), but the radiant distributions in the fainter range cannot be obtained by photography and CCD. Figure 32 shows the image intensifier radiants during the Taurid activity period and it is clear the distribution is similar as for the radar observations in Figure 33. Fainter Taurids show no distinct separation into two components and they are largely hidden in the sporadic background except for the time of the maximum.

The CCD radiant distribution is shown in Figure 30, and in this figure, except for the Geminids, both branches of the Taurids are clearly recorded. The Southern branch starts earlier and ends sooner than the Northern one. The Southern branch is located further from the ecliptic plane than the Northern branch. This CCD distribution compares very well with the photographic results.

Figures 31 and 34 show the distribution of the Taurids' perihelia for photographic and CCD observations respectively. The CCD distributions are divided into six sub-period groups shown above. It is noteworthy to mention that:

1. The perihelion distribution is elongated along the ecliptic plane and suggests that the orbital plane of the Taurids rotates about the ecliptic axis and not that of 2P/Encke.

2. The perihelion of the 'Northern branch' at the maximum almost coincides with 2P/Encke's.

3. The perihelion of the 'Southern branch' at the maximum recedes in the distance relative to 2P/Encke's.

2.2 α-Capricornids

Shigeno's Australia expeditions revealed the very unique nature of the so-called α-Capricornids (Shigeno & Shigeno, 2004). Former photographic and visual observations claim that the α-Capricornids are rich in bright meteors including fireballs. But the image intensifier observations are quite contrary to our common ideas (see Section 1.6 δ-Aquariids in this article).

Ecliptic radiants obtained from the Southern hemisphere observations by image intensifiers are shown in Figure 25 and the α-Capricornids are distributed in the range of $170 \leq \lambda - \lambda_\odot < 185$ and $+8 \leq \beta < +18$. The center of the distribution is located about $\lambda - \lambda_\odot = 177$ and $\beta = +12$ (Figure 36), slightly northwestward of the photographic α-Capricornids (Figure 35). CCD observations by Ueda (Figure 37) suggest that their radiant points concentrate between the image intensifier radiants and the center of photographic observations, but a little bit closer to the image intensifier center.

The radiant distribution and the recorded number of meteors for the geocentric velocity distribution plotted against solar longitude suggest that the α-Capricornids display one continuous activity, however these observations are mainly during the later half of the α-Capricornid activity (Figures 38 and 39). The CCD observations seem to indicate that the α-Capricornid stream is active for longer than formerly reported. The image intensifier observations show a slower geocentric velocity than the photographic and the CCD observations as well as a decline with time. The radiant- and velocity distribution as a function of time obtained from the image intensifier data suggests that this 'α-Capricornid stream' is another one and needs future work.

The radiant distribution and the recorded number of meteors for the geocentric velocity distribution versus solar longitude for photographic data might suggest that 'α-Capricornids' consist of two components (Figure 38). Lindblad (1971) detected two components but his minor component could not be recognized in the image intensifier radiants. His major component may consist of two components and one of them could coincide with the image intensifier α-Capricornids.

This 'faint α-Capricornid stream' could be a different one from the so-called 'α-Capricornids'. But, the distribution of their perihelia shows that they overlap each other (Figure 40). It is so complex in the ecliptic activity region that we need future work if we want to declare the 'α-Capricornids' as established.

3 What is the critical definition of a meteor shower: case of Comae Berenicids

It is proper to use photographic data to check the continuity of meteor activity because the photographic observations were carried out over a longer operation period than the radar observations. We define the target area as $230 \leq \lambda - \lambda_\odot < 255$ and $+10 \leq \beta < +30$ for the so-called Comae Berenicid photographic meteors (Koseki, 2009).

Figure 41 shows the geocentric velocity (km/s) distribution plotted against solar longitude for the photographic candidate meteors observed during the whole year. Meteor activity continues over this time with some slight concentrations but these may be caused by observational biases or dips.

Figure 43 shows the photographic geocentric velocity (km/s) distribution in this area for the interval $200 \leq \lambda_\odot < 310$, when the activity in this area seems to reach a peak. We could divide them into the following five groups according to this figure and to the corresponding figures for the CCD and image intensifier observations (see Table 13).

Points in Figure 44 distinguish several clusters in this period and show a slight concentration about $\lambda - \lambda_\odot = 243$ and $\beta = +20$. However individual meteors disperse widely with vague centers. Does this concentration mean that the Comae Berenicids are false or that they are lasting barely over three months from a single radiating area?

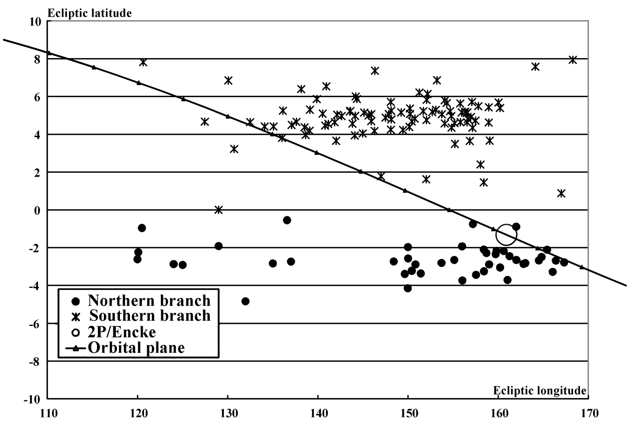

Figure 31 – The perihelion distributions for photographic 'Taurids' in ecliptic coordinates.

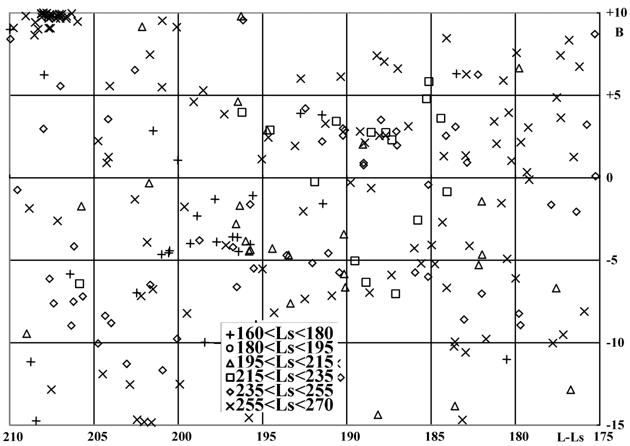

Figure 32 – Radiant distribution for image intensifier observations during the activity period of the Taurids shown in six separate periods.

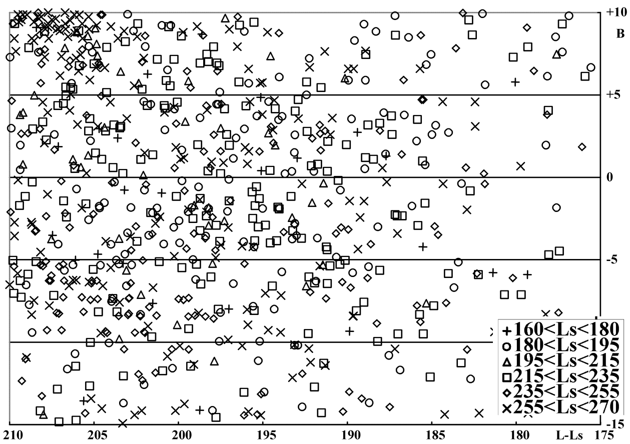

Figure 33 – Radiant distribution for radar observations during the activity period of the Taurids shown in six separate periods.

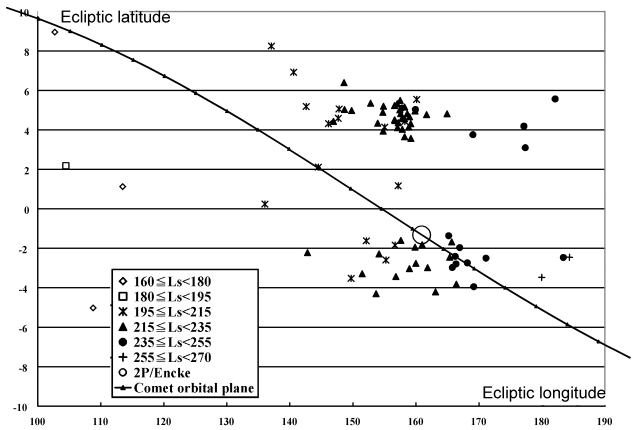

Figure 34 – The perihelion distributions for CCD 'Taurids' in ecliptic coordinates shown in six separate periods.

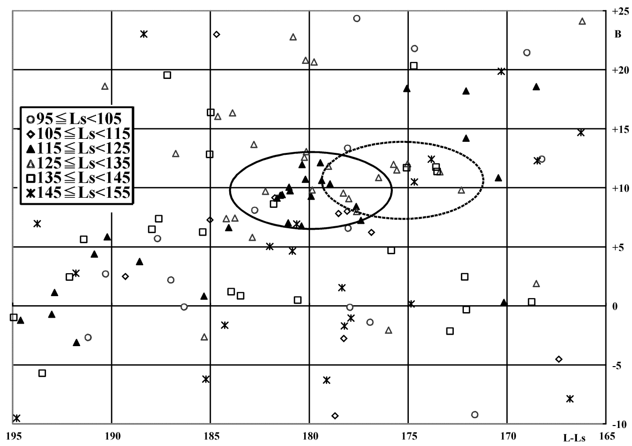

Figure 35 – Photographic 'α-Capricornid' radiant point distribution.

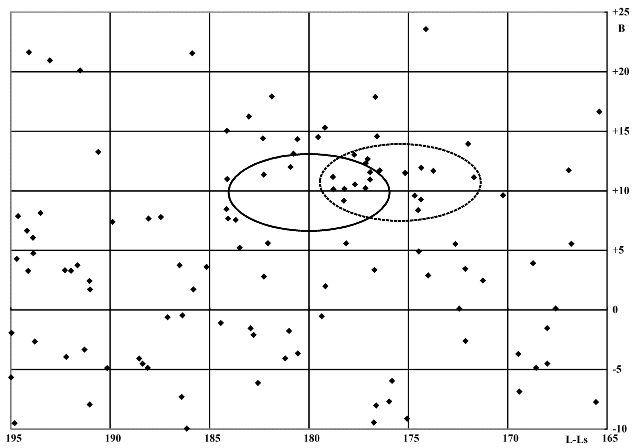

Figure 36 – Image intensifier 'α-Capricornid' radiant point distribution.

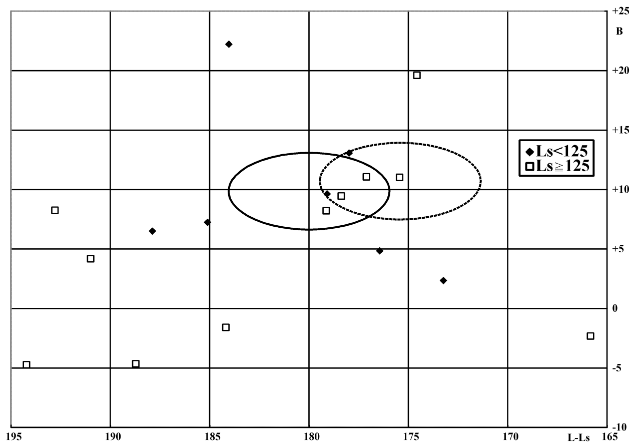

Figure 37 – CCD 'α-Capricornid' radiant point distribution.

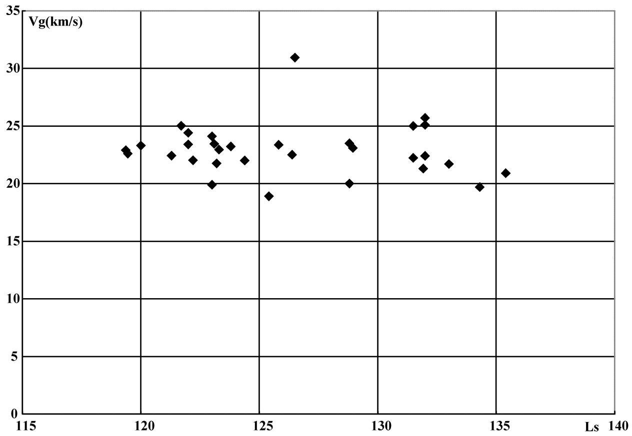

Figure 38 – Geocentric velocity distribution for photographed α-Capricornids.

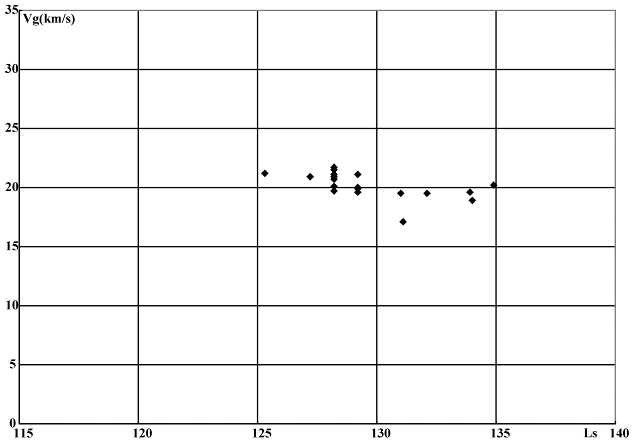

Figure 39 – Geocentric velocity distribution for α-Capricornids recorded by image intensifier.

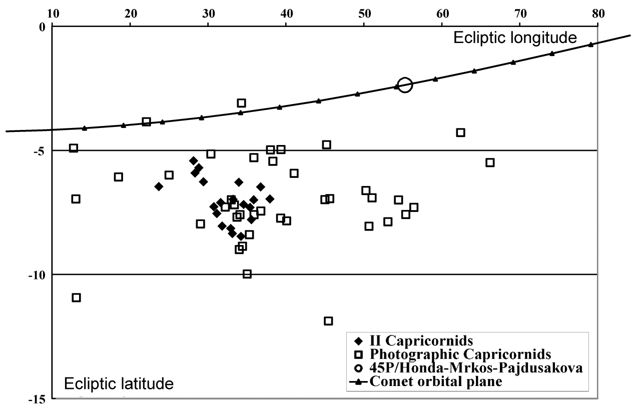

Figure 40 – The perihelion distributions for the 'α-Capricornids' in ecliptic coordinates.

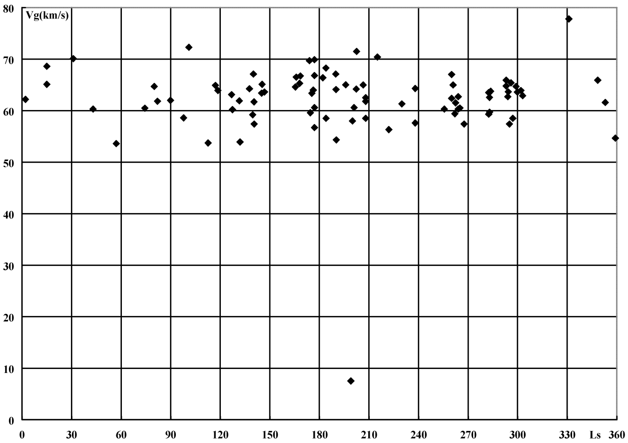

Figure 41 – Meteor activity for the 'Comae Berenicids' area, set as $230 \leq \lambda - \lambda_\odot < 255$ and $+10 \leq \beta < +30$, shown by the geocentric velocity distribution during the year, by photographic observations.

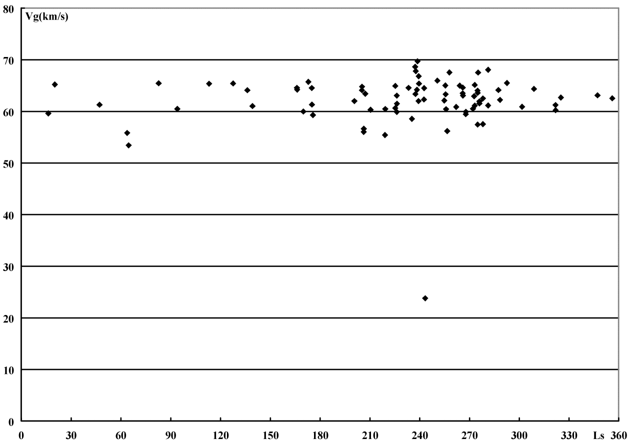

Figure 42 – Meteor activity for the 'Comae Berenicids' area, set as $230 \leq \lambda - \lambda_\odot < 255$ and $+10 \leq \beta < +30$, shown by the geocentric velocity distribution during the year, by CCD observations.

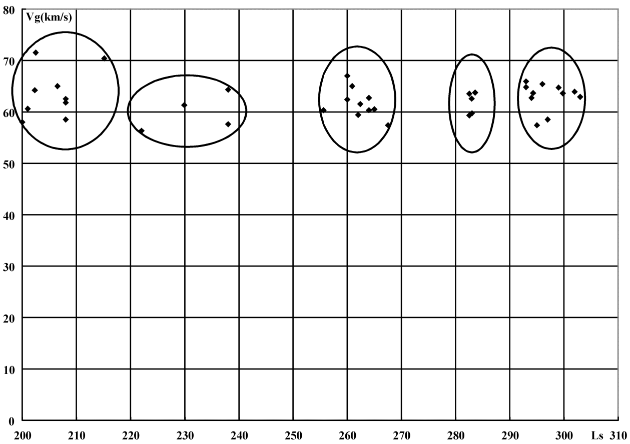

Figure 43 – Five 'Comae Berenicid' candidates with the activity assumed from the geocentric velocity distribution from photographic observations.

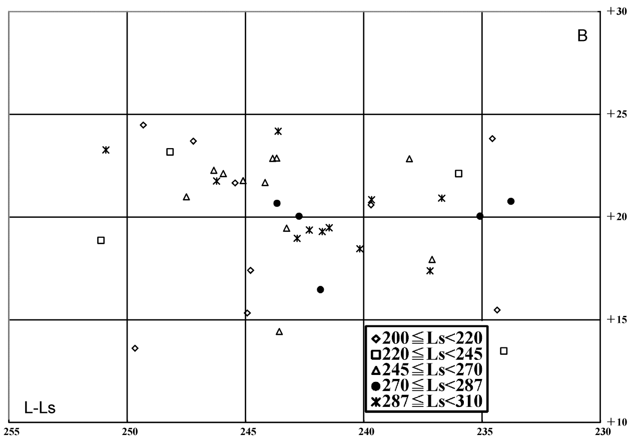

Figure 44 – Radiant point distributions of the 'Comae Berenicid' candidates in ecliptic coordinates shown in five separate periods.

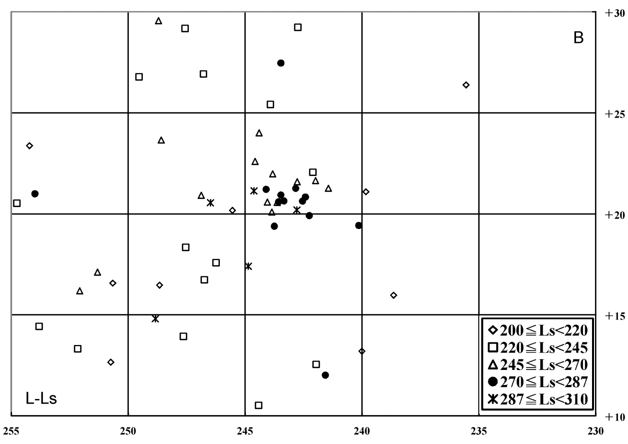

Figure 45 – Radiant point distributions of the 'Comae Berenicid' candidates in ecliptic coordinates shown in five separate periods, based on CCD observations.

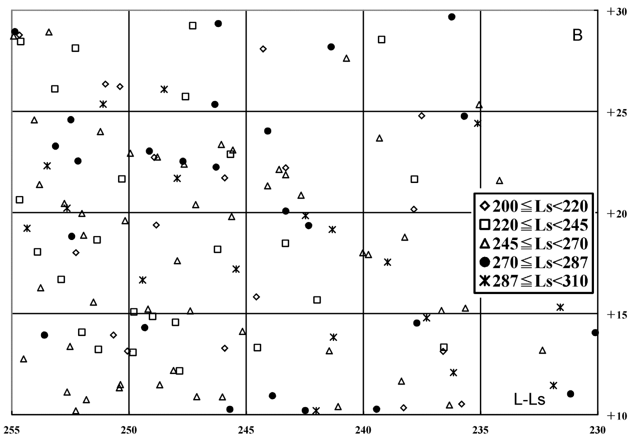

Figure 46 – Radiant point distributions of the 'Comae Berenicid' candidates in ecliptic coordinates shown in five separate periods, based on image intensifier observations.

Table 13 – Meteor activity around the 'Comae Berenicids' area.

Group I	$200 \leq \lambda_\odot < 220$
Group II	$220 \leq \lambda_\odot < 245$
Group III	$245 \leq \lambda_\odot < 270$
Group IV	$270 \leq \lambda_\odot < 287$
Group V	$287 \leq \lambda_\odot < 310$

Ueda's CCD results give a similar activity profile (Figure 42) and a similar radiant concentration for the interval $200 \leq \lambda_\odot < 310$ (Figure 45). The five clusters in the geocentric velocity distributions are not clear when compared to the photographic results but the center of the radiants seems more distinct than for the photographs. Meteors during the interval $270 \leq \lambda_\odot < 287$ display a distinct concentration around $\lambda - \lambda_\odot = 243$ and $\beta = +20$ in good agreement with the photographic indication. So did the CCD observations capture the Comae Berenicids?

Shigeno's image intensifier observations complicate the matter, that is, the image intensifier meteors do not show a concentration in any area (Figure 46). In addition to this, radar results show no indication of radiant groups. Meteor activity in this area may be rich in the brighter range and rather poor in fainter meteors observable by image intensifiers and radar.

Visual observations (Koseki, 2009) show a similar profile like CCD observations, that is, the radiants seem to concentrate around $\lambda - \lambda_\odot = 240$ and $\beta = +20$, and the activity declines towards January. There might be some meteor activity but it is not clear if it is a single one or some composites. The activities may show different profiles from CCD to image intensifiers as well as visual to radar.

4 Why do we need different methods to observe meteors?

It should be emphasized that the two video devices have unique properties and that they have different advantages. In short, image intensifiers can observe the faintest meteors in optical observations and CCD allows us to record meteors while we are asleep. Image intensifiers are suitable to study the faint meteor population but not for continuous observing. CCD is good to survey poor but bright meteor activity lasting for many days but not to register faint and short meteors.

There are several other observing techniques to study meteors such as naked eye, telescope, photography and radar (radio) and each of these has different properties too. It is necessary to treat the results obtained by different methods very carefully in order to avoid erroneous conclusions. Visual observers and radio observers may record quite different meteor activities.

References

Koseki M. (2009). "Meteor shower records: A reference table of observations from previous centuries". *WGN, Journal of the IMO*, **37**, 139–160.

Koseki M., Ueda M., and Shigeno Y. (2010a). "What is the difference between image intensifier and CCD meteor observations? I. CCD and image intensifier observations in Japan". *WGN, Journal of the IMO*, **38**, 99–107.

Koseki M., Ueda M., and Shigeno Y. (2010b). "What is the difference between image intensifier and CCD meteor observations? II. Comparison of the results". *WGN, Journal of the IMO*, **38**, 118–122.

Lindblad B. (1971). "A computerized stream search among 2401 photographic meteor orbits". *Smithsonian Contributions to Astrophysics*, **12**, 14–24.

McCrosky R. E. and Posen A. (1961). "Orbital elements of photographic meteors". *Smithsonian Contributions to Astrophysics*, **4**, 15–84.

Shigeno Y. and Shigeno T. (2004). "Radiant distributions of the Capricornid-Aquarid complex". *WGN, Journal of the IMO*, **32**, 77–80.

Shigeno Y., Toda M., and Shioi H. (1997). "Double-station observations of the Eta-Aquarids". *WGN, Journal of the IMO*, **25**, 217–221.

Southworth R. and Hawkins G. (1963). "Statistics of meteor streams". *Smithsonian Contributions to Astrophysics*, **7**, 261–285.

Handling Editor: Paul Roggemans

Meteor activity from the Perseus-Auriga region in September and October

Jürgen Rendtel [1] *and Sirko Molau* [2]

A systematic search was carried out for radiants of high-inclination meteor showers in September and October based on data collected over eleven years with cameras of the IMO Video Meteor Network. The Aurigids (206 AUR), with an outburst in 2007, and the September ε-Perseids (208 SPE), with an outburst in 2008, were the most prominent showers. Detailed SPE outburst data of 2008 are presented. Data of the October Lyncids (228 OLY) and the β-Aurigids (210 BAU) stored in the database of the IAU Meteor Data Center have been confirmed. Radiant data of the September Lyncids (81 SLY) have been improved, and the activity period of the δ-Aurigids (224 DAU) has been better defined. Two new radiants have been detected: the September-October Lyncids (424 SOL) and the ψ-Aurigids (425 PSA). All showers are at high-inclination orbits and may be part of a complex which could be similar to the Kreutz group of comets.

Received 2010 August 20

1 Introduction

In the detailed analysis of video meteor data published in August 2009 (Molau & Rendtel, 2009) the radiants in the Perseus-Auriga region in September and October were excluded because of their complex appearance. In that paper we described the most prominent showers from this region, the Aurigids (206 AUR) and the September ε-Perseids (208 SPE). Further, the September Lyncids (81 SLY) were associated with one of the radiants found active for only three data bins.

The case of these high-inclination showers was also selected for a separate paper because of the probable existence of more than two showers in that region and in the specified period. Meteor activity from that region has been the subject of earlier analyses. Those analyses focussed on the question of the relation between the September Perseids as described by Hoffmeister (1948) and the δ-Aurigids found by Drummond (1982). In the IMO meteor shower working list, these two showers were put together for many years as their radiant and velocity data allowed them to be considered as one continuous source (Rendtel, 1993). Later, Dubietis & Arlt (2002) found arguments that these should be considered two independent sources, with the September Perseids being active mainly around September 9 and the δ-Aurigids being detectable in early October with a period of very low activity around 190° Solar longitude. However, the radiant position found from modern data (video as well as visual) strongly suggested that the activity in (early) September occurs from a radiant which is at a different position from the previously listed September Perseid radiant. This was strongly supported when an unexpected outburst was observed on 2008 September 9, from a radiant which fits with the September ε-Perseids (208 SPE), which is about 10° off from the (former) September Perseid radiant (Jenniskens, 2008). The outburst observed on 2008 September 9 was centered at 08^h20^m UT (±20 min) and lasted for about four hours (Jenniskens, 2008; Molau & Kac, 2008). Most meteors were in the magnitude range between +4 and −8. Table 1 gives a summary of observations around the September Perseid outburst; a preliminary analysis of the radiant position and activity profile was published by Molau & Kac (2008).

For the present analysis we added further video data obtained to the sample used for the previous paper (Molau & Rendtel, 2009) and repeated the analysis for the period between 150° and 215° in Solar longitude (corresponding to August 23 – October 29). The total sample for this interval contains 168 830 meteors. The number of meteors per bin of 2° length varies from a low of 1328 meteors (at 191°) to a high of 6000 meteors (at 208° – the Orionid maximum).

When looking for possible radiants in the Perseus-Auriga region in the sky, we have to carefully distinguish them from the activity coming from the diffuse Northern Apex source (Campbell-Brown & Jones, 2006; SonotaCo, 2009). These apex meteors have velocities which are quite similar to the high-inclination showers.

As in the previous analysis, we refer to the data stored in the files of the IAU Commission 22 Meteor Data Center (IAU MDC) data base and also use the respective designation. All data presented here, has been confirmed by the IAU Commission 22 working group for shower designation.

2 Confirmation of radiants from the IAU data base

First, we checked the radiant and activity data for the Aurigids (206 AUR) and the September-ε Perseids (208 SPE), which we easily detected in the data sample. Both showers have produced activity outbursts within the ten years of the video camera network operation (cf. Rendtel, 2007, for the 206 AUR and Table 1 for the 208 SPE). Results for these two showers were listed in the previous paper (Molau & Rendtel, 2009), and the position and drift can be seen in Figure 1. We can also confirm the detection of the October Lyncids (228 OLY). The data fit the entry in the IAU MDC data base. The activity occurs only in the last portion of the interval and can be found in Figure 3.

[1] Eschenweg 16, 14476 Potsdam & Astrophys. Inst. Potsdam, An der Sternwarte 16, 14482 Potsdam, Germany
Email: jrendtel@aip.de
[2] Abenstalstr. 13, 84072 Seysdorf, Germany
Email: sirko@molau.de

IMO bibcode WGN-385-rendtel-peraur
NASA-ADS bibcode 2010JIMO...38..161R

Table 1 – Observational data of the period centered around the September ε-Perseid outburst on 2008 September 9, covering the period from September 8 (evening) to September 10 (morning). An activity profile derived from complete data of the IMO Video Meteor Network was published by Molau & Kac (2008). The video data listed below is just to characterize the size of the sample.

Period UT	SPE meteors	Lim. magn.	Method	Location	Observer	Reference
1853–2300 2300–0200 0200–0342	2 2 3	≈ 4	video (Sep 08–09)	near Venice, Italy 12.1°E, 45.6°N	E. Stomeo	Stomeo, 2008
2300–0130	8	6.3	visual (Sep 08–09)	Viernau, Germany 10.5°E, 50.7°N	P. Bader	Rendtel, 2008
0058–0248	4	6.2	visual	Potsdam, Germany 13.0°E, 52.5°N	J. Rendtel	Rendtel, 2008
0455–0555 0600–0700 0700–0800 0800–0900 0900–0945	4 2 9 16 5	5.7 5.7 5.8 5.8 5.6	visual	Ames, Iowa, USA 93.6°W, 42.1°N	P. Martsching	Martsching, 2008
0620–1030	25 brighter -2		all-sky video	Marshall Space Flight Center, 97°W, 38°N	W.J. Cooke	Jenniskens, 2008
0726–0921	11		wide-field camera low-light-level video	Kelowna, BC, Canada 119.5°W 49.9°N	J. Brower	Jenniskens, 2008
0732–1047	14	≈ 2	video	Tucson, Arizona, USA 111°W, 32°N	C. Hergenrother	Hergenrother, 2008
0700–1200	4	6.0	video	San Diego, USA 117.1°W, 32.1°N	R. Lunsford	Molau & Kac, 2008
0718–1005	"increased rate"		forward met. scatter	Helsinki, Finland 25°E, 60°N	E. Lyytinen	Jenniskens, 2008
2245–0055	0	6.2	visual (Sep 09–10)	Potsdam, Germany 13.0°E, 52.4°N	S. Näther	Rendtel, 2008
2357–0215	6	6.2	visual (Sep 09–10)	Potsdam, Germany 13.0°E, 52.5°N	J. Rendtel	Rendtel, 2008

Two further weak sources listed in the IAU MDC data base can probably be associated with radiants derived from our data: between September 17 and 19 (174°–176°) we find a radiant at $\alpha = 43°, \delta = +65°$ with $V_\infty = 54$ km/s. This is not far from the position given for the September β-Cassiopeids (207 SCS). However, both the radiant and the velocity do not fit well and we would not have recognized the case if it were not in the data base. We did not check the coincidence in further detail as the source is away from the region we focussed on.

Another radiant at $\alpha = 87°, \delta = +49°$ with $V_\infty = 70$ km/s fits nicely with the β-Aurigids (210 BAU) for which the IAU MDC gives $\alpha = 86°, \delta = +43°$ at 67 km/s. Like the previous case, this weak source can be detected only over three bins between 179° and 181° (September 22–25). Its drift is included in Figure 2.

3 Delta Aurigids and radiants in Lynx

The initial question was whether there is a continuous activity from the Perseus-Auriga region starting with the shower listed as 208 SPE, becoming the 224 DAU (δ-Aurigids) later in September and October. The δ-Aurigids were discussed in detail by Drummond (1982) and because of the similarity with the activity in early September these were considered as coming from one source (Rendtel, 1993). Analyses of observations later indicated that there are two distinct sources (Dubietis & Arlt, 2002).

From the updated video meteor data we checked the activity from the Northern Apex source which is not too far from the region. This source forms no defined radiant but rather a scattered area from which meteors occur on retrograde orbits (Campbell-Brown & Jones, 2006). The size of this region may have a radius of about 10°. Thus any distinct source should be about 20° away from the (average) North Apex source center. We determined this source also from our data and calculated a mean center and its average drift over the entire period. At this point we checked for possible other sources.

First, we come back to the case of the September Lyncids (81 SLY). Already in our previous analysis (Molau & Rendtel, 2009) we stated that this is a weak source of short duration which can be detected only over three bins. Since the data for the entry in the IAU MDC data base was of low accuracy, we decided to assign the activity found in our data with the entry in the data base. Now, the present analysis shows two weak sources. In the interval 165–173° we find a radiant at $\alpha = 111°, \delta = +56°$ at 59 km/s which fits well to the current entry in the IAU MDC data base $(107°, +55°, 61$ km/s). We suggest that this should remain the 81 SLY entry (see Figure 1). The short duration shower found in the 2009 analysis—which was then associated with the 81 SLY—is different as we find $\alpha = 110°, \delta = +48$ at $V_\infty = 68$ km/s. Unfortunately, this is also in the constellation Lynx with few and no named stars. Hence it is now September-October-Lyncids (424 SOL, shown in Figure 2) because both the September Lyncids (81 SLY) and the October Lyncids (228 OLY) were already listed. Their radiants and drifts occur in Figures 1 and 3, respectively.

With the δ-Aurigids, we again find two radiants which both are more than 20° away from the Apex and also that distance from each other. Both radiants deviate from the data listed in the IAU MDC. At 191° Solar longitude – given as the maximum of the shower 224 DAU, our data show nothing in the respective region. The two sources we can detect occur later. The more western radiant fits reasonably with the 224 DAU data if extrapolated. We suggest a change in the entry for the 224 DAU and the addition of a radiant which is named ψ-Aurigids (425 PSA). The respective data are listed in Table 2, and the positions can be seen in Figure 3. Possibly, the two radiants we find from the present video data were not separated in the previous analyses – although this would not explain the difference in the activity data.

4 Rejected sources

Three more radiants have been detected from our data. They are all closer to the apex than the 20 degree limit mentioned in section 3. Further, the associated activity expressed in the rate VR strongly varies between neighbouring bins, indicating that the data do not represent a reliable source. Finally, the deviation between radiant positions calculated for successive bins also exceeds the limits set in our 2009 paper.

5 Conclusions

There are several weak sources producing activity from the region between Perseus, Lynx and Auriga. In the case of the first of the stronger showers, the Aurigids (206 AUR), the parent comet C/1911 N1 (Kiess) is confirmed. The radiant and activity of the September ε-Perseids (208 SPE) is also well established, at least after the activity outburst observed in 2008, although a parent object is not yet known. Further weak showers with radiants in the same region are the δ-Aurigids (224 DAU) which are definitely separate from the September ε-Perseids (208 SPE). Three radiants in the constellation Lynx were found. They do not form a continuous source as their positions in the sky differ significantly in declination. This becomes obvious in the summarizing Figure 4. The September-October-Lyncids (424 SOL) are a new detection. The two showers in Auriga, the β-Aurigids (210 BAU) and the newly detected ψ-Aurigids (425 PSA) are of short duration (detected over three and five bins, respectively). Except for the peculiar Aurigids (206 AUR), no parent objects are known. Perhaps all or some of these showers $(130° < i < 150°)$ result from a group of comets on highly inclined orbits, somewhat similar to the Kreutz group.

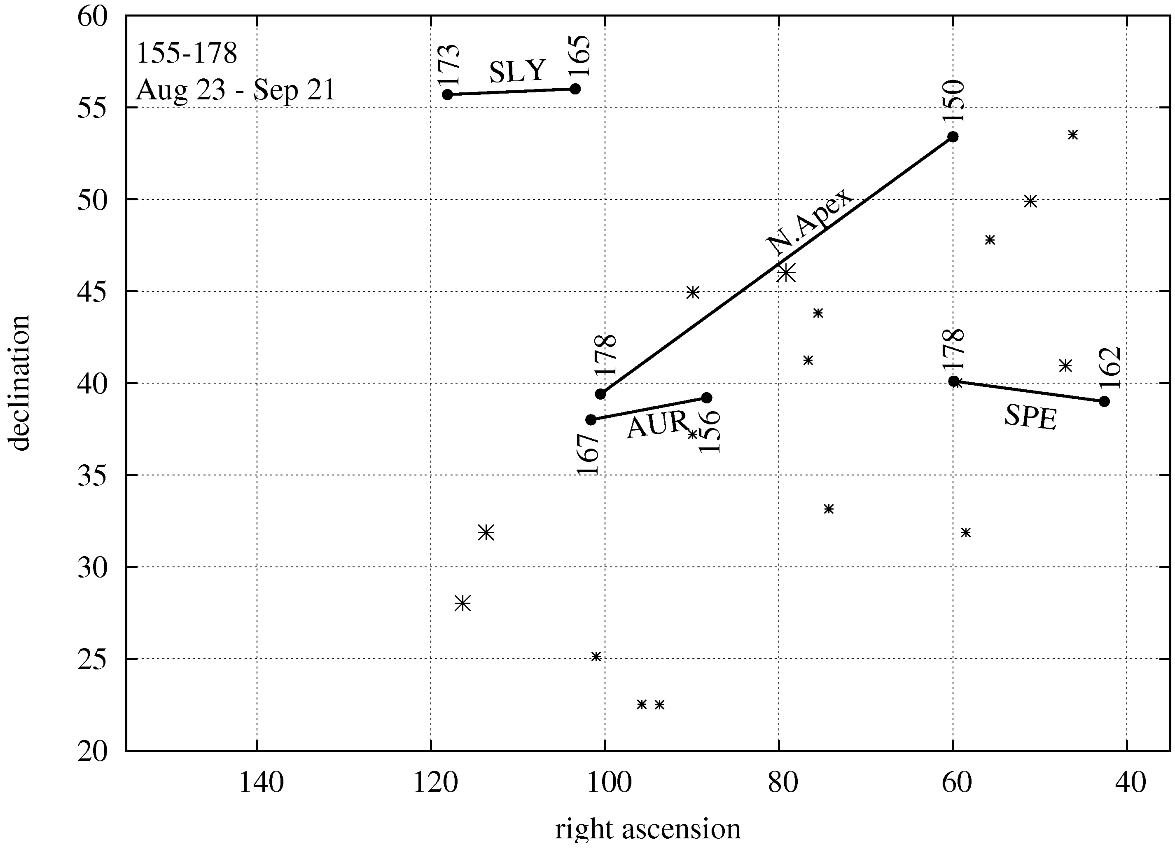

Figure 1 – Radiants in the Perseus-Auriga region in the period 155–178°. Here we find two considerable showers and the Northern Apex source. The numbers along the radiant drifts denote the corresponding Solar longitudes. Bright stars of Perseus, Auriga and Gemini are shown as asterisks.

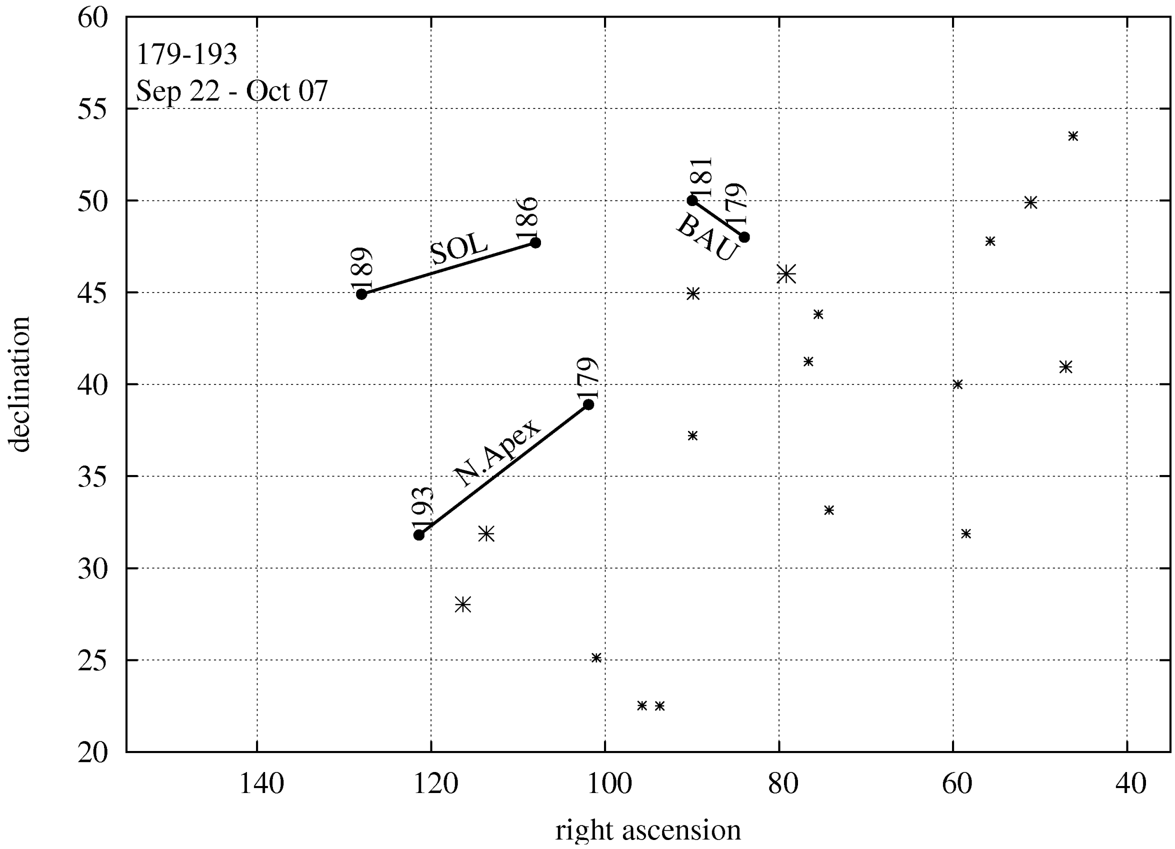

Figure 2 – Radiants in the Perseus-Auriga region in the 179–193° period. The numbers along the radiant drifts denote the corresponding Solar longitudes.

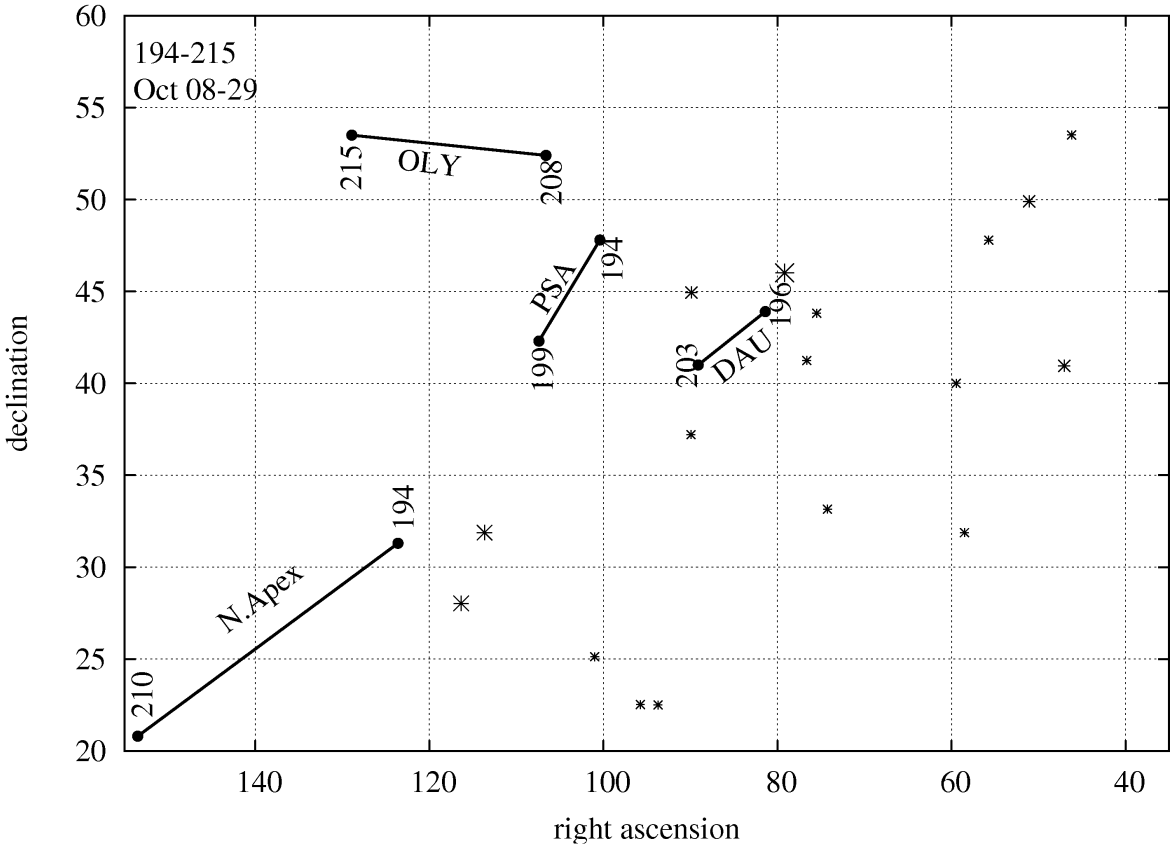

Figure 3 – Radiants in the Perseus-Auriga region in the 194–215° period. The numbers along the radiant drifts denote the corresponding Solar longitudes.

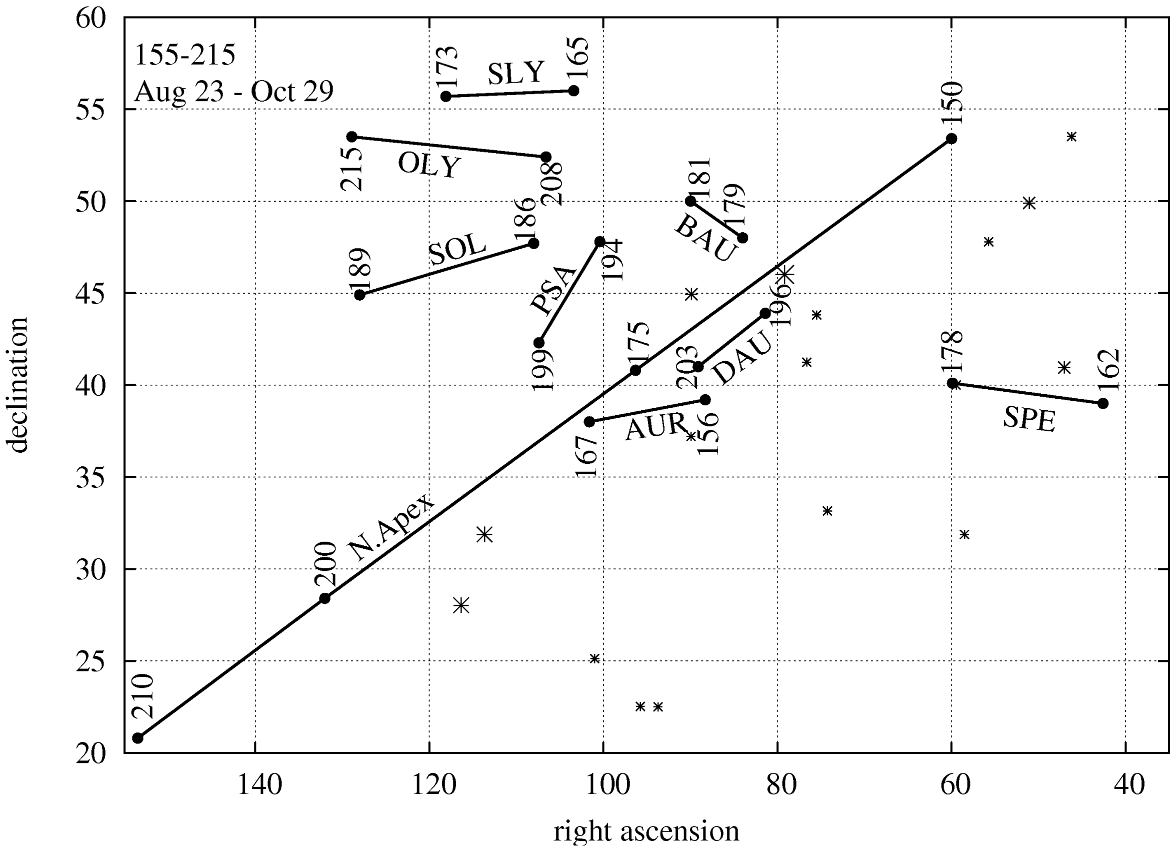

Figure 4 – All radiants in the Perseus-Auriga region which were detected during the entire period under study. The numbers along the radiant drifts denote the corresponding Solar longitudes, the three-letter codes refer to the IAU meteor shower designation.

Table 2 – Data of the meteor showers discussed in this paper sorted by Solar longitude (J2000.0). (V) refers to the obtained video data, (L) gives the values of the MDC list. VR is the video rate (explained by Molau & Rendtel, 2009). The last column gives the number of meteors associated with the shower radiant. Information for the Northern Apex source found from the video meteor data are given for comparison.

Shower	Peak $\lambda_\odot$[°]		Period $\lambda_\odot$[°]	Rad. position and drift [°]				V_∞ [km/s]		Max.	Meteors
	(V)	(L)	(V)	α	$\Delta\alpha$	δ	$\Delta\delta$	(V)	(L)	VR	
206 AUR	159	158	156–167	93	+1.1	+39	−0.1	67	67	3.0	1128
208 SPE	167	170	162–178	48	+1.1	+40	+0.1	66	65	3.3	1930
81 SLY	169	167	165–173	111	+1.8	+56	−0.0	59	62	1.8	530
210 BAU	180	179	179–181	87	+3.1	+49	+1.2	70	67	1.8	559
424 SOL	186	–	186–189	110	−2.9	+48	−0.7	68	–	1.6	237
224 DAU	198	191	196–203	84	+1.1	+44	−0.4	67	66	1.7	744
425 PSA	199	–	194–199	107	+1.4	+42	−1.1	69	–	2.0	602
228 OLY	210	206	208–215	113	+3.2	+53	+0.2	61	66	1.3	516
N.Apex			150–215		+1.4		−0.5	68	68		2408

References

Campbell-Brown M. and Jones J. (2006). "Annual variation of sporadic meteor rates". *MNRAS*, **367**, 709–716.

Drummond J. (1982). "A note on the Delta Aurigid meteor stream". *Icarus*, **51**, 655–659.

Dubietis A. and Arlt R. (2002). "The current Delta-Aurigid meteor shower". *WGN, Journal of the IMO*, **30**, 168–174.

Hergenrother C. (2008). "September Perseids – 2008/09/09 – prelim video results". `http://lists.meteorobs.org/pipermail/meteorobs/2008-September/008844.html`. Meteorobs mailing list, message 008844 (Sep. 9, 2008).

Hoffmeister C. (1948). *Meteorströme*. J.A. Barth, Leipzig.

Jenniskens P. (2008). "September Perseid meteors 2008". *Electronic Telegram No. 1501, Central Bureau for Astronomical Telegrams.* (Sep. 9, 2008).

Martsching P. (2008). "Sept Perseids 08/09 Sept 2008". `http://lists.meteorobs.org/pipermail/meteorobs/2008-September/008847.html`. Meteorobs mailing list, message 008847 (Sep. 9, 2008).

Molau S. and Kac J. (2008). "Results of the IMO Video Meteor Network – September 2008". *WGN, Journal of the IMO*, **36**, 112–113.

Molau S. and Rendtel J. (2009). "A comprehensive list of meteor showers obtained from 10 years of observations with the IMO Video Meteor Network". *WGN, Journal of the IMO*, **37**, 98–121.

Rendtel J. (1993). "Radiant and orbits of δ-Aurigids and September Perseids". In Očenáš D. and Zimnikoval P., editors, *Proceedings of the IMC Smolenice 1992*, pages 67–73. IMO.

Rendtel J. (2007). "Visual observations of the Aurigid peak on 2007 September 1". *WGN, Journal of the IMO*, **35**, 108–112.

Rendtel J. (2008). "Visuelle Meteorbeobachtungen im September 2008". *Meteoros*, **11**, 190–191.

SonotaCo (2009). "A meteor shower catalog based on video observations in 2007–2008". *WGN, Journal of the IMO*, **37**, 55–62.

Stomeo E. (2008). "September Perseids". `http://lists.meteorobs.org/pipermail/meteorobs/2008-September/008855.html`. Meteorobs mailing list, message 008855 (Sep. 10, 2008).

Handling Editor: Javor Kac

Results of the IMO Video Meteor Network — July 2010

Sirko Molau [1] *and Javor Kac* [2]

The IMO Video Meteor Network cameras observed for almost 2 600 hours of effective observing time and recorded more than 13 000 meteors in 2010 July. The activity of July meteor showers has been studied. The July Pegasids were active above the sporadic background from July 8 to 16. The α-Capricornids reached their maximum between July 26 and 29. The activity of Southern δ-Aquariids rose sharply after July 24; their maximum could not be accurately determined due to insufficient data from July 28 to 30. Enhanced activity of the Perseids from July 14 to 16 was detected on top of the steadily rising profile. Extended functions of MetRec are also described.

Received 2010 August 26

1 Introduction

The favorable observing conditions of the previous month continued in July. It is therefore no surprise that 17 cameras obtained meteor records in more than twenty observing nights. Stefano Crivello even managed to record during all July nights with his camera Stg38. In total, we collected more than 13 000 meteors in almost 2 600 hours of effective observing time and missed only slightly the July record of last year (Table 1 and Figure 1). The data of three cameras are still missing though.

As usual, meteor activity increased significantly in the middle of the month. The combination of longer nights with upcoming activity of the Perseids and southern meteor showers resulted in higher meteor counts. The monthly average increased from 3.4 meteors per hour in June to 5.2 in July. Our Australian observer Steve Kerr was particularly successful again. In the last few days of July and the first few days of August he recorded more Southern δ-Aquariids than many European observers record Perseids in the middle of August!

Once more, we could integrate a new camera in our network. Hupol (a Mintron camera with 3.8 mm $f/0.8$ lens) is operated south-west of Lake Balaton by two members of the Nagykanizsa Astronomical Association and further completes the Hungarian camera network.

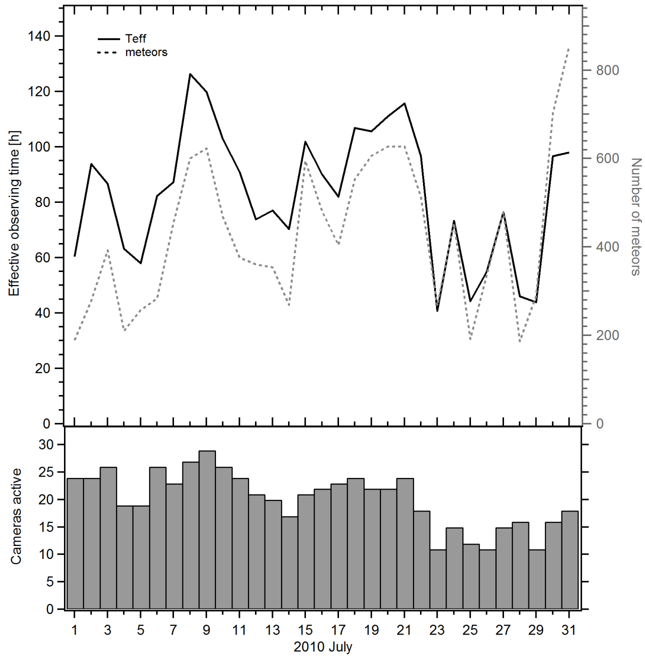

Figure 1 – Monthly summary for the effective observing time (solid black line), number of meteors (dashed gray line) and number of cameras active (bars) in 2010 July.

2 Unusual activity of July Pegasids and the Perseids

Two observers reported unusual activity in July again. First, Christoph Gerber noted increased rates of the July Pegasids during his visual observation on July 8/9. A few days later, Enrico Stomeo reported unusual Perseid activity in the Italian video data from July 14/15 to 16/17. In the following nights, the Perseids almost disappeared again.

To confirm these observations, we accumulated the number of shower meteors over all cameras for each night, and divided them by the number of sporadic meteors. To check the rates in particular near the start of the activity intervals, we recomputed the meteor shower assignment beforehand as if all relevant showers were active in all of July. In addition, we omitted the data from Steve Kerr for this analysis as they affected the Southern δ-Aquariids too much. The resulting profiles are given in Figure 2. Beside the rates for individual showers, the absolute number of sporadic meteors is given in the background, to document the size of the data set for each night.

In the first few nights of July, all four showers have activity values near 0.05. Recent analyses have shown that this is approximately the level of the sporadic background (i.e. of sporadic meteors that match by chance to a meteor shower radiant). Hence, the analyzed showers were not visible in these nights.

According to our long-term analysis of last year, the July Pegasids are active from July 7 to 29. Their rate profile shows only small variations in the full activity interval, such that the maximum on July 10 is hardly noticeable. This year, the July Pegasids emerged from the background around July 8 and remained active at a low level until July 16. There are no hints for enhanced July Pegasid activity on July 8/9.

[1] Abenstalstr. 13b, 84072 Seysdorf, Germany.
Email: sirko@molau.de
[2] Na Ajdov hrib 24, 2310 Slovenska Bistrica, Slovenia.
Email: javor.kac@orion-drustvo.si

IMO bibcode WGN-385-molau-vidjul
NASA-ADS bibcode 2010JIMO...38..167M

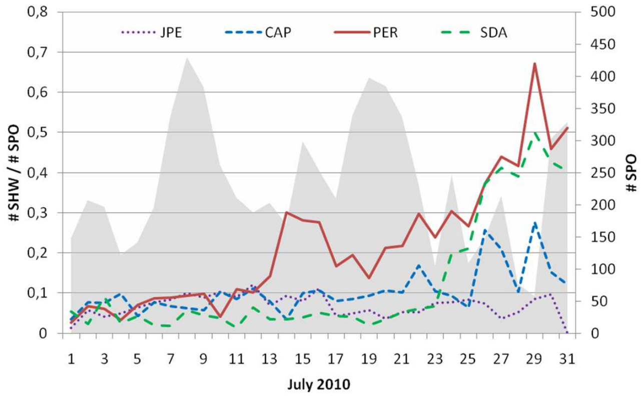

Figure 2 – Activity profile of the July Pegasids, α-Capricornids, Perseids, and Southern δ-Aquariids in July 2010. Plotted is the number shower meteors per night, divided by the number of sporadics. The absolute number of sporadic meteors is given in the background.

Next, the α-Capricornids became noticeable around July 10. Their activity level remained low as well. Only between July 26 to 28 the number of Capricornids was significantly higher. That matches well to the maximum we found in last year's analysis (July 28; see Molau & Kac, 2009). The additional peak on July 29/30 may have been caused by insufficient data, because both the Perseids and Aquariids showed unusually high rates that night as well.

The Perseids became visible around July 11/12. That was earlier than what we found in our recent analysis, when we set the start date to July 14 (Molau & Rendtel, 2009). As noted by Enrico (Stomeo, 2010), the rate in the three nights July 14/15 to 16/17 was indeed unusually high – the number of Perseids increased by about a factor of two. If the sporadic background is taken into account, the activity level might have been even a factor of three higher than usual. In the following nights, the rates went back to normal and reached the same level only on July 22 to 26. As the data set was sufficiently large in all nights, we assume that the rate increase is real. It might be an interesting task for theorists to find the reason for this activity peak at the start of the Perseid activity interval.

Finally, the Southern δ-Aquariids became noticeable on July 24/25. Their activity rose strongly in the following days, and they soon reached the same shower meteor counts as the Perseids. However, due to their southern radiant position, the observing conditions for the Aquariids are much worse in the northern hemisphere than for the Perseids. Hence, their ZHR was in fact more than twice as high as the Perseid ZHR. According to our long-term analysis, the maximum of the Southern δ-Aquariids occurs on July 30. From the 2010 data, the maximum time cannot be determined because of insufficient data on July 28/29 and 29/30.

3 MetRec

As noted before, the Southern δ-Aquariids are much more prominent in the Australian data. On July 31, for example, Steve Kerr recorded 86 meteors of this shower, 63 sporadics, but only two Perseids. To combine data from both hemispheres in a sensible way, it is necessary to consider the observing geometry. The activity profiles presented in our 2009 analysis were based on the observability function, which expresses how long and at what altitude a meteor shower radiant is visible at a certain observing site. The figures were also scaled by the number of sporadic meteors, as neither the effective observing time, nor the limiting magnitude, field of view and other basic camera parameters were known. To have better analysis options in the future, MetRec was extended in June by two important functions. First, the software computes the limiting magnitude in the active field of view each minute and stores it in an extra text file. In the past, often only longer gaps in meteor detection hinted at partial cloud coverage. Now we have a detailed limiting magnitude profile for each night that shows clearly when the observing conditions deteriorate in-between or when the sky is fully clouded. In the second step, the collection area is determined for each camera. For that, the effective field of view is computed in square degrees, and converted into square kilometers at the meteor layer at 85 km altitude. This value is corrected for the distance to the observer (absolute magnitude) and the extinction: The lower a camera points to the horizon, the larger is the atmospheric surface it covers, but the more distant and therefore fainter are the meteors. The larger atmospheric volume near the horizon reduces the brightness further. By combining the collection area with the limiting magnitude of the camera (assuming a population index r of 2.5) and the observing time, we obtain the effective collection area. That value is measured in $\mathrm{km}^2 \times \mathrm{h}/\mathrm{r}^{(6.5-\mathrm{mag})}$ and reflects the power of a meteor camera much better than the plain observing time. For simplicity, we will only use the term $\mathrm{km}^2 \times \mathrm{h}$ from now on.

For demonstration, we compare the July results of two different meteor cameras. The first one is the image-intensified camera Avis2 with a 50 mm $f/1.4$ lens. It has a roughly circular field of view of 60 degrees diameter and yields a limiting magnitude of 6 magnitude. The camera points north of the zenith and covers a collection area of almost 1 800 square degrees, or 6 100 square kilometers. If that value is corrected by the distance of the meteor layer and the extinction, the effective collection area is reduced to 4 400 km^2.

The second camera is Mincam1, a relatively old Mintron camera that is equipped with a 12 mm $f/0.8$ lens and yields a limiting magnitude of 4.5 magnitude. This camera covers a surface of almost 1 500 square degrees. It points lower to the horizon in south-eastern direction, which results in a collection area of 42 000 square kilometers. This figure reduces to 5 400 after correcting for distance and extinction.

Let us now take the data from July 31. The effective observing time of Avis2 was 4.7 hours, in which 71 meteors were recorded. The effective collection area was roughly 8 100 $\mathrm{km}^2 \times \mathrm{h}$. Mincam1 was operated for 6.8 hours, but recorded only 45 meteors. The lower number of detected meteors can be explained by the smaller effective collection area – only about 6 000 $\mathrm{km}^2 \times \mathrm{h}$.

Figure 3 shows the number of meteors divided by

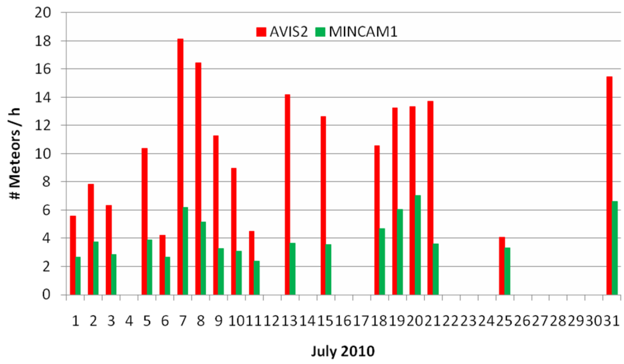

Figure 3 – Number of meteors for both cameras Avis2 and Mincam1 in July, divided by the effective observing time in the corresponding night.

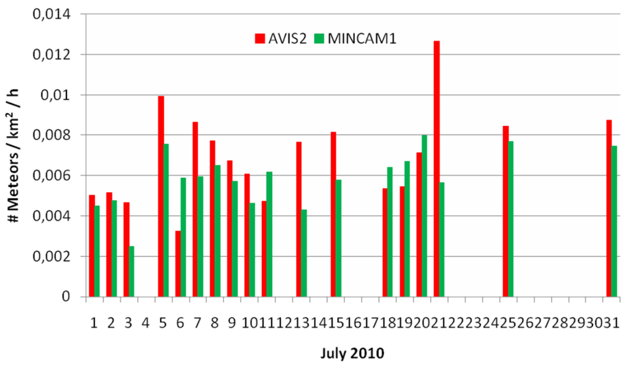

Figure 4 – Number of meteors for both cameras Avis2 and Mincam1 in July, divided by the effective collection area in the corresponding night.

the effective observing time for both cameras in July. As expected, Avis2 recorded clearly more meteors per hour than Mincam1, and the hourly rate deviates significantly from one night to the next due to the variable observing conditions. In Figure 4, the number of meteors is divided by the effective collection area. Here, both cameras perform equally well, and the deviations from one night to the next are much smaller. In total, the effective collection area of Avis2 in the given July nights was 123 000 km^2 × h (with 855 meteors), and that of Mincam1 was 58 000 km^2 × h (with 349 meteors).

Of course, the correction is not yet perfect, but a large fraction of the camera dependencies are removed by the new method, and we get a step closer to measurements of fluxes from video data. More about this method was presented at the IMC 2010 in Armagh.

Figure 5 – IMO Video Meteor Network camera Armefa, stationed in Berlin.

Figure 6 – Meteor video cameras at Armagh Observatory (three cameras in back). In front is the three-camera system of the Polar Bear Telescope.

References

Molau S. and Kac J. (2009). "Results of the IMO Video Meteor Network – July 2009". *WGN, Journal of the International Meteor Organization*, **37:5**, 164–167.

Molau S. and Rendtel J. (2009). "A comprehensive list of meteor showers obtained from 10 years of observations with the IMO video meteor network". *WGN, Journal of the International Meteor Organization*, **37:4**, 98–121.

Stomeo E. (2010). "Remarkable activity of Perseids on July?". `http://lists.meteorobs.org/pipermail/meteorobs/2010-July/012253.html` . Meteorobs mailing list, message 12253 (2010 July 22).

Handling Editor: Javor Kac

Table 1 – Observers contributing to 2010 July data of the IMO Video Meteor Network.

Code	Name	Place	Camera	FOV	LM	Nights	Time (h)	Meteors
BENOR	Benitez-S.	Las Palmas	TIMES4 (1.4/50)	⊘ 20°	3 mag	10	17.5	50
BRIBE	Brinkmann	Herne	HERMINE (0.8/6)	⊘ 55°	3 mag	24	87.3	303
CRIST	Crivello	Valbrevenna	C3P8 (0.8/3.8)	⊘ 80°	3 mag	28	132.5	613
			STG38 (0.8/3.8)	⊘ 80°	3 mag	31	124.3	436
ELTMA	Eltri	Venezia	MET38 (0.8/3.8)	⊘ 80°	3 mag	22	102.5	434
GONRU	Goncalves	Tomar	TEMPLAR1 (0.8/6)	⊘ 55°	3 mag	28	157.8	917
			TEMPLAR2 (0.8/6)	⊘ 55°	3 mag	28	102.0	424
GOVMI	Govedič	Središče ob Dravi	ORION2 (0.8/8)	⊘ 42°	4 mag	17	62.8	240
HERCA	Hergenrother	Tucson	SALSA2 (1.2/4)	⊘ 80°	3 mag	18	38.9	116
HINWO	Hinz	Brannenburg	AKM2 (0.85/25)	⊘ 32°	6 mag	14	55.8	217
IGAAN	Igaz	Budapest	HUPOL (0.8/3.8)	⊘ 80°	3 mag	22	67.2	192
JOBKL	Jobse	Oostkapelle	BETSY2 (1.2/85)	⊘ 25°	7 mag	13	49.6	626
KACJA	Kac	Kostanjevec	METKA (0.8/8)	⊘ 42°	4 mag	1	0.3	1
		Ljubljana	ORION1 (0.8/8)	⊘ 42°	4 mag	22	79.2	254
		Kamnik	REZIKA (0.8/6)	⊘ 55°	3 mag	12	60.0	336
			STEFKA (0.8/3.8)	⊘ 80°	3 mag	14	52.6	239
KERST	Kerr	Glenlee	GOCAM1 (0.8/3.8)	⊘ 80°	3 mag	23	197.4	1797
MOLSI	Molau	Seysdorf	AVIS2 (1.4/50)	⊘ 60°	6 mag	18	76.7	855
			MINCAM1 (0.8/8)	⊘ 42°	4 mag	22	91.5	377
		Ketzür	REMO1 (0.8/3.8)	⊘ 80°	3 mag	25	82.0	239
			REMO2 (0.8/3.8)	⊘ 80°	3 mag	26	97.6	410
MORJO	Morvai	Fülöpszallas	HUFUL (0.8/3.8)	⊘ 80°	3 mag	10	35.0	79
OCHPA	Ochner	Albiano	ALBIANO (1.2/4.5)	⊘ 68°	3 mag	2	7.3	15
PERCZ	Perko	Becsehely	HUBEC (0.8/3.8)	⊘ 80°	3 mag	5	25.5	92
ROBBI	Roberto	Verona	FIAMENE (0.8/3.8)	⊘ 80°	3 mag	5	20.9	93
ROTEC	Rothenberg	Berlin	ARMEFA (0.8/6)	⊘ 55°	3 mag	16	53.6	209
SCHHA	Schremmer	Niederkrüchten	DORAEMON (0.8/3.8)	⊘ 80°	3 mag	26	73.0	211
SLAST	Slavec	Ljubljana	KAYAK1 (1.8/28)	⊘ 50°	4 mag	18	63.1	188
STOEN	Stomeo	Scorze	MIN38 (0.8/3.8)	⊘ 80°	3 mag	22	124.5	801
			NOA38 (0.8/3.8)	⊘ 80°	3 mag	21	121.7	799
			SCO38 (0.8/3.8)	⊘ 80°	3 mag	21	122.0	973
STRJO	Strunk	Herford	MINCAM2 (0.8/6)	⊘ 55°	3 mag	11	24.8	71
			MINCAM3 (0.8/8)	⊘ 42°	4 mag	15	38.2	129
			MINCAM5 (0.8/6)	⊘ 55°	3 mag	13	34.6	135
TEPIS	Tepliczky	Budapest	HUMOB (0.8/3.8)	⊘ 80°	3 mag	23	96.4	411
					Overall	31	2 576.1	13 282

Results of the IMO Video Meteor Network — August 2010

Sirko Molau [1] *and Javor Kac* [2]

August 2010 was a new record month for the IMO Video Meteor Network: more than 50 cameras were active during the month, collecting more than 4 500 hours of effective observing time and almost 32 500 meteors. New MetRec functions are explained and some examples given. Activity profiles of the Perseids, Southern δ-Aquariids, and α-Capricornids are presented throughout July and August.

Received 2010 October 8

1 Introduction

Astronomical conditions were perfect in August 2010 – the Perseid maximum fell during the European night time hours of August 12/13, right after the new Moon. All that was needed was the right weather. There were marvelous observing conditions indeed – but not at all observing sites. More southern locations experienced perfect conditions, whereas more northern observers were often hampered by clouds. There was a total of 25 cameras with twenty or more observing nights and often well above 100 hours of effective observing time, whereas other automated cameras gathered only about 50 hours.

The camera network grew a little further in August. Erno Berko has joined the network with a new station in northern Hungary. For the first time we reached a total of 50 active video systems. At the same time, we managed to surpass the record breaking output of August 2009 by a few percent. With more than 4 500 hours of effective observing time and 32 500 meteors, August 2010 now ranks first in the long-term statistics of the IMO network (Table 1 and Figure 1).

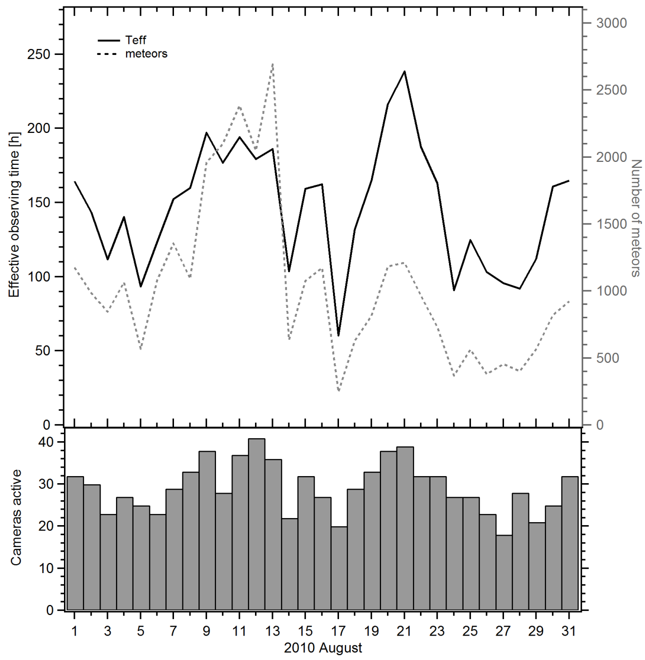

Figure 1 – Monthly summary for the effective observing time (solid black line), number of meteors (dashed gray line) and number of cameras active (bars) in 2010 August.

2 New MetRec features applied

As reported in the previous month, a new version of MetRec was introduced in July that allows measurement of both the limiting magnitude and the effective collection area (Molau & Kac, 2010). Some observers have used this software version already in August so that we can now present first results from a larger set of cameras. For this purpose, the observer overview (Table 1) was reworked.

At first, the field of view (in square degrees) was calculated for each camera. Cameras with an active field of view that is smaller than the size of the video frame (e.g. the circular FOV of an image intensifier) are marked with an asterisk. In these cases, only the active field of view was measured.

It is expected that cameras with identical objective lenses and without obstruction have the same field of view, which is apparently not the case. For thirteen cameras with the 3.8 mm Computar lens, the field of view varies between 5 537 and 5 632 square degrees, for example. The average is 5 598 ± 32. The variations result from inaccuracies in the determination of the plate constants, which yields noticeable deviations at the edges of the field of view. However, the variations are smaller than they appear at first glance, as the field of view is a square measure. If the cameras had a square field of view, the edge length would be 74.8 ± 0.2 degrees. So the error is well below one percent. Similar variations are observed for lenses with longer focal length.

On average, the following values were obtained for the most common Computar lenses:

Focal length [mm]	2.6	3.8	6	8	12
Number of cameras	1	13	8	3	2
Field of view [square degrees]	6636	5598	2352	1456	735

In this paper the individual values are reported in Table 1. In the future only the average values will be given there.

The collection area is obtained from the field of view. Based on the observing direction of the camera the number of square kilometers the field of view covers at 100 km altitude is calculated (discussions at the recent IMC have shown that this norm altitude is more sensible than the previously used 85 kilometers). The collection area is corrected for the absolute meteor

[1]Abenstalstr. 13b, 84072 Seysdorf, Germany. Email: sirko@molau.de
[2]Na Ajdov hrib 24, 2310 Slovenska Bistrica, Slovenia. Email: javor.kac@orion-drustvo.si

IMO bibcode WGN-385-molau-vidaug
NASA-ADS bibcode 2010JIMO...38..171M

magnitude and the extinction, i.e. the reduced limiting magnitude for meteors near the horizon (due to the larger distance from the observer and extinction) is converted into a corrected collection area. The corrected collection area varies by two orders of magnitude from 200 square kilometers for a camera with 50 mm lens to over 25 000 square kilometers for cameras with a 2.6 or 3.8 mm lens. The average is about 13 000 square kilometers.

The collection area alone does not yet fully characterize the performance of a camera – for that, the limiting magnitude has to be considered as well. A camera with a smaller collection area but very good limiting magnitude can record more meteors than a camera with a larger collection area but a smaller limiting magnitude. For those cameras that used already the new software version in August, Table 1 gives the best stellar limiting magnitudes measured in reality. The values vary between about 3.5 and 6 mag, where image-intensified cameras and those with longer focus lenses naturally have better values.

The effective collection area is finally corrected for the difference in limiting magnitude to 6.5 mag. That is, the effective collection area is getting smaller, the lower the limiting magnitude of the camera. The population index r plays an important role. It describes by what factor the number of meteors increases when the limiting magnitude improves by one magnitude. At this time, a value of $r = 2.5$ is used. The effective collection area of a camera with a limiting magnitude of 6.5 mag is left unchanged, for a camera with 5.5 mag it decreases by a factor of 2.5 (down to 40%), and for a camera with 4.5 mag it decreases by a factor of 2.5^2 (down to 16%).

The effective collection areas calculated this way and given in Table 1 represent the real efficiency of the meteor camera under good observing conditions. The values range from almost 1 000 up to 4 500 square kilometers of effective collection area (normalized to 6.5 mag). As expected, the highest values are achieved by image-intensified cameras. However, the gap between these and the best non-intensified cameras is smaller than observed in reality (based on meteor counts). Thus, the real average population index will be larger than 2.5.

Finally, in addition to the effective observing time, Table 1 contains the effective collection area accumulated over time (measured in thousand $\mathrm{km}^2 \times \mathrm{h}$). As most cameras switched to the new software version at some time in August, the existing measures were extrapolated to the total effective observing time. The given value reflects not just the efficiency of the camera (collection area, sensitivity), but also the real observing conditions, i.e. how long each camera could observe at the respective site under what conditions (real limiting magnitude). The values vary between 50 000 and 300 000 $\mathrm{km}^2 \times \mathrm{h}$ in August. Primary factor was the difference in observing conditions mentioned earlier which presented to some sites almost three times more clear skies than to other sites.

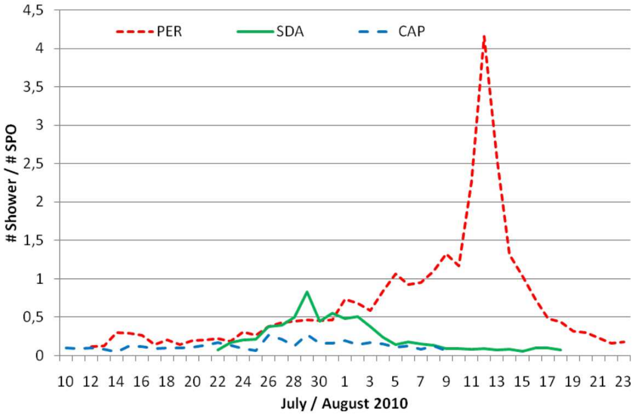

Figure 2 – Activity profile of the Perseids, Southern δ-Aquariids and α-Capricornids in July/August 2010. Displayed is the number of shower meteors divided by the number of sporadics per night.

Note that these are all first analysis results for the different cameras. They help us to better understand the different camera systems and observing sites, and to verify the new software functions. In some cases the parameter choice was not yet perfect, so that the quality of the derived figures will further improve in the future.

3 Preliminary results for the Perseids, Southern δ-Aquariids and α-Capricornids

After these considerations with respect to camera efficiency, we shall have a short view on the overall meteor activity of the major showers. Figure 2 gives the combined activity profiles for the Perseids (13 300 meteors), Southern δ-Aquariids (2 100 meteors) and α-Capricornids (1 300 meteors) in July and August. Thanks to the size of our camera network, we can now derive activity profiles of individual showers each year. Further improved data quality is expected when the scaling of shower meteor counts is not anymore based on sporadic meteors, but on the effective collection area per night.

References

Molau S. and Kac J. (2010). "Results of the IMO Video Meteor Network – July 2010". *WGN, Journal of the International Meteor Organization*, **38:5**, 167–170.

Handling Editor: Javor Kac

Table 1 – Observers contributing to 2010 August data of the IMO Video Meteor Network. Eff.CA designates the effective collection area and Tot.CA the total collection area.

Code	Name	Place	Camera	FOV [°²]	Stellar LM [mag]	Eff.CA [km²]	Nights	Time [h]	Tot.CA [10³km²h]	Meteors
BENOR	Benitez-S.	Las Palmas	TIMES4 (1.4/50)	2359	—	—	7	12.9	—	50
			TIMES5 (0.95/50)	33	—	—	2	2.6	—	9
BERER	Berko	Ludanyhalaszi	HULUD (1.0/2.6)	6638	—	—	8	38.7	—	228
BRIBE	Brinkmann	Herne	HERMINE (0.8/6)	2374	—	—	25	109.1	—	613
CASFL	Castellani	Monte Baldo	BMH1 (0.8/6)	2350	—	—	30	138.8	—	471
			BMH2 (1.2/4.5)*	4243	—	—	29	173.9	—	863
CRIST	Crivello	Valbrevenna	C3P8 (0.8/3.8)	5575	—	—	22	123.1	—	803
			STG38 (0.8/3.8)	5593	—	—	29	162.5	—	1112
ELTMA	Eltri	Venezia	MET38 (0.8/3.8)	5620	—	—	28	168.8	—	921
GONRU	Goncalves	Tomar	TEMPLAR1 (0.8/6)*	2188	5.3	2331	26	172.8	266.2	1195
			TEMPLAR2 (0.8/6)*	2303	5.0	2397	26	164.9	308.8	879
GOVMI	Govedič	Središče ob Dravi	ORION2 (0.8/8)	1471	6.0	3916	21	116.5	187.4	960
HERCA	Hergenrother	Tucson	SALSA2 (1.2/4)	2900	—	—	2	1.6	—	8
			SALSA3 (1.2/4)*	4332	4.0	1471	26	128.6	150.8	750
HINWO	Hinz	Brannenburg	AKM2 (0.85/25)*	754	5.7	1306	12	49.9	49.7	257
IGAAN	Igaz	Baja	HUBAJ (0.8/3.8)	5600	4.3	3338	16	90.4	272.2	499
		Hodmezovasarhely	HUHOD (0.8/3.8)	5609	4.2	3031	19	97.1	189.6	451
		Budapest	HUPOL (1.2/4)	3929	3.5	1144	23	102.5	71.9	404
JOBKL	Jobse	Oostkapelle	BETSY2 (1.2/85)*	1725	—	—	12	64.8	—	852
KACJA	Kac	Kostanjevec	METKA (0.8/8)*	1381	4.0	2246	12	63.9	60.2	269
		Ljubljana	ORION1 (0.8/8)	1420	5.3	2336	28	132.8	147.5	957
		Kamnik	REZIKA (0.8/6)	2307	5.0	2293	20	91.6	—	911
			STEFKA (0.8/3.8)	5540	4.2	2882	19	78.4	151.9	556
KERST	Kerr	Glenlee	GOCAM1 (0.8/3.8)	5238	4.0	2215	24	186.2	—	2007
KOSDE	Koschny	Noordwijkerhout	LIC1 (1.4/50)*	2038	5.7	3123	5	13.9	—	264
			LIC4 (1.4/50)*	2027	—	—	11	47.5	—	580
			TEC1 (1.4/12)	741	—	—	9	32.7	—	98
LUNRO	Lunsford	Chula Vista	BOCAM (1.4/50)*	1860	—	—	1	4.3	—	294

Table 1 – Observers contributing to 2010 August data of the IMO Video Meteor Network – continued from previous page.

Code	Name	Place	Camera	FOV [°2]	Stellar LM [mag]	Eff.CA [km^2]	Nights	Time [h]	Tot.CA [10^3km^{2}h]	Meteors
MOLSI	Molau	Seysdorf	AVIS2 (1.4/50)*	1771	6.1	4182	10	38.6	85.5	662
			MINCAM1 (0.8/8)	1477	4.9	1716	22	101.6	101.7	624
		Ketzür	REMO1 (0.8/3.8)	5592	3.0	974	18	66.2	49.8	257
			REMO2 (0.8/3.8)	5635	4.3	2846	17	64.7	93.7	299
MORJO	Morvai	Fülöpszallas	HUFUL (1.4/5)	2522	—	—	25	105.0	—	386
OCHPA	Ochner	Albiano	ALBIANO (1.2/4.5)	1971	—	—	26	73.9	—	153
OTTMI	Otte	Pearl City	ORIE1 (1.4/16)	3837	—	—	21	125.1	—	644
PERCZ	Perko	Becsehely	HUBEC (0.8/3.8)*	5448	3.4	1500	23	114.5	103.5	857
ROBBI	Roberto	Verona	FIAMENE (0.8/3.8)	5632	—	—	26	146.2	—	643
ROTEC	Rothenberg	Berlin	ARMEFA (0.8/6)	2369	—	—	19	76.8	—	440
SCHHA	Schremmer	Niederkrüchten	DORAEMON (0.8/3.8)	5537	—	—	21	93.7	—	447
SLAST	Slavec	Ljubljana	KAYAK1 (1.8/28)	596	—	—	22	98.1	—	473
STOEN	Stomeo	Scorze	MIN38 (0.8/3.8)	5631	—	—	27	177.6	—	1818
			NOA38 (0.8/3.8)	5609	—	—	27	171.4	—	1762
			SCO38 (0.8/3.8)	5598	—	—	27	183.3	—	2059
STORO	Stork	Kunžak	KUN1 (1.4/50)*	1913	5.4	2778	3	18.1	—	722
		Ondřejov	OND1 (1.4/50)*	2195	5.8	4595	3	19.9	—	747
STRJO	Strunk	Herford	MINCAM2 (0.8/6)	2357	—	—	15	49.2	—	226
			MINCAM3 (0.8/12)	728	—	—	13	41.8	—	224
			MINCAM5 (0.8/6)	2344	—	—	16	51.9	—	405
TEPIS	Tepliczky	Budapest	HUMOB (0.8/6)	2375	4.9	2258	17	103.5	134.7	951
YRJIL	Yrjölä	Kuusankoski	FINEXCAM (0.8/6)	2337	—	—	17	61.4	—	449
					Overall	31	4 553.3	—	32 497	

* active field of view smaller than video frame

The International Meteor Organization

web site http://www.imo.net

IMO Sales

Available from the Treasurer or the Electronic Shop on the IMO Website	€	$
IMO membership, including subscription to WGN Vol. 38 (2010)		
Surface mail	26	39
Air Mail (outside Europe only)	49	69
Electronic subscription only	21	29
Back issues of WGN on paper		
Vols. 26 (1998) – 37 (2009) except 30 (2002), per complete volume	15	23
Vol. 37 (2009) – electronic version only	9	13
Proceedings of the International Meteor Conference on paper		
1990, 1991, 1993, 1995, 1996, 1999, 2000, 2002, 2003, per year	9	13
2005, 2006, 2008	15	23
Proceedings of the Meteor Orbit Determination Workshop 2006	15	23
Proceedings of the Radio Meteor School 2005 on paper	15	23
Handbook for Meteor Observers	20	29
Electronic media		
Meteor Beliefs Project CD-ROM	5	7
DVD: WGN Vols. 6–30 & IMC 1991, 1993–96, 2001–04	45	69